# Quantitative analysis of extensional joints in the southern Adriatic foreland (Italy), and the active tectonics of the Apulia region

D. Di Bucci [a,*], R. Caputo [b], G. Mastronuzzi [c], U. Fracassi [d], G. Selleri [e], P. Sansò [e]

[a] *Dipartimento della Protezione Civile. Via Vitorchiano, 4 – 00189 Roma, Italy*
[b] *Università degli Studi di Ferrara, Dipartimento di Scienze della Terra. Via Saragat, 1 – 44100 Ferrara, Italy*
[c] *Università degli Studi di Bari, Dipartimento di Geologia e Geofisica. Via Orabona, 4 – 70125 Bari, Italy*
[d] *Istituto Nazionale di Geofisica e Vulcanologia. Via di Vigna Murata, 605 – 00143 Roma, Italy*
[e] *Università degli Studi di Lecce, Dipartimento di Scienza dei Materiali. Via per Arnesano – 73100 Lecce, Italy*

*** Corresponding Author:**
Daniela Di Bucci
Dipartimento della Protezione Civile
Via Vitorchiano, 4
00189 - Roma, Italy
Tel.: ++39-06-68204761
Fax: ++39-06-68202877
e-mail: daniela.dibucci@protezionecivile.it

**Running title** Adriatic foreland active tectonics

## Abstract

The Adriatic foreland of the Apennines comes ashore only in Apulia (easternmost Italy). Its southern part, our study area, lacks any structural analysis devoted to define its recent-to-active tectonics. Throughout the Quaternary, this region was affected by mild brittle deformation with rare faults, characterized by small displacement, and widespread extension joints, frequently organized in sets. Therefore, we conducted a quantitative and systematic analysis of the joint sets affecting Quaternary deposits, by applying an inversion technique *ad hoc* to infer the orientation and ratio of the principal stress axes, $R = (\sigma_2 - \sigma_3)/(\sigma_1 - \sigma_3)$. Within a general extensional regime, we recognized three deformational events of regional significance. The oldest event, constrained to the early and middle part of the Middle Pleistocene, is characterized by variable direction of extension and R between 0.64-0.99. The penultimate event, dated late Middle Pleistocene, is characterized by an almost uniaxial tension, with a horizontal $\sigma_3$ striking ~N43°E; R is high, between 0.85-0.99. The most recent event is characterized by the lowermost R values, that never exceed 0.47 and are frequently <0.30, indicating a sort of horizontal 'radial' extension. This event is not older than the Late Pleistocene and possibly reflects the active stress field still dominating the entire study area.

**Keywords:** Quaternary tectonics, brittle deformation, fracture, Pleistocene

## 1. Introduction

The foreland of the Apennines fold-and-thrust belt (Italy) corresponds essentially to the Adriatic Sea (Fig. 1), that has long been considered a tectonically and seismically "stable" area. Only in its central sector, this foreland is characterized by significant historical and instrumental seismicity (Gruppo di Lavoro CPTI, 2004; Castello et al., 2005; Fig. 2), both off-shore (active Mesoadriatic strip; Console et al., 1993) and on-land (Molise-Gondola shear zone; Di Bucci et al., 2006; Fig. 1), and some seismogenic faults have already been identified (DISS Working Group, 2007, and references therein; Di Bucci et al., 2009b).

This foreland is exposed on-land only in the easternmost sector of the Italian peninsula, i.e. in the Apulia region (Fig. 1). Northern Apulia is the locus of rare but destructive historical earthquakes (Gruppo di Lavoro CPTI, 2004), occasionally associated with surface faulting (Piccardi, 2005) and possibly with coseismic uplift of limited parts of the coastal area (Mastronuzzi and Sansò, 2002a). The Tyrrhenian (MIS 5.5, ~125 ka) coastline is variously displaced from the Ionian side to the Adriatic one, indicating inhomogeneous tectonic behaviour during the Late Pleistocene (e.g. Bordoni and Valensise, 1998; Ferranti et al., 2006). Seismites have been recognized in Upper Pleistocene deposits along the southern Adriatic coasts, testifying to the occurrence of strong ground shaking, that has been associated with Late Pleistocene earthquakes located within a ~40 km distance from the seismites outcrops (Tropeano et al., 1997; Fig. 3). In contrast, only one moderate historical earthquake occurred in Southern Apulia (1826 Manduria earthquake, Imax=VI-VII, M=5.3; Gruppo di Lavoro CPTI, 2004; Fig. 2). Indeed, in 1743 the southern portion of the Adriatic foreland was hit by a severe earthquake sequence (which also triggered a tsunami; Mastronuzzi and Sansò, 2004; Tinti et al., 2004; Mastronuzzi et al., 2007a), but these events have been positively located off-shore (Imax=IX-X, M=6.9; Gruppo di Lavoro CPTI, 2004; Guidoboni and Ferrari, 2004).

On the one hand, this brief overview can explain why the active geodynamics of the Adriatic block is still debated. In the lack of a shared interpretation, different models have been proposed, among which the buckling of a thick continental lithosphere, either within an active subduction beneath the Southern Apennines or due to horizontal compression, or the NW-SE Eurasia-Nubia convergence. On the other hand, this overview also suggests that Southern Apulia, a region whose recent deformation was never investigated from a mesostructural point of view, is in need of a detailed analysis that may help to outline its recent tectonic evolution and its present-day deformation regime. Preliminary results of an original structural analysis carried out with this purpose indicate that Middle and Late Pleistocene deposits in Southern Apulia have been affected by mild but recurrent and discernible brittle deformation (Di Bucci et al., 2009a). Faults are rare and all characterized by small displacement values, whereas extension joints prevail in most of the investigated sites, they are frequently well exposed and organized in sets. The occurrence of this mild tectonic deformation, and the lack of a significant number of shear planes (even of faults at the mesoscale) affecting Quaternary deposits, led us to approach the identification of the causative stress field by an in-depth quantitative analysis of the joint sets and of their relationships with one another. Here we present the results of this innovative approach, which was never attempted before for the characterization of the active deformation of the southern Adriatic foreland.

## 2. Geology of Apulia

### *2.1. Tectonic outline*

The Adriatic foreland is shared among key fold-and-thrust belts of the Central Mediterranean, i.e., the Albanides, the Dinarides, and the Apennines of peninsular Italy. Apennines are a Late Cenozoic-Quaternary accretionary wedge, which forms part of the Africa-verging mountain system in the Alpine-Mediterranean area. In the Southern Apennines, this wedge is formed by east-to-northeast verging thrust sheets deriving from palaeogeographic domains of alternating carbonate platforms and pelagic basins (e.g. Mostardini and Merlini, 1986; Patacca and Scandone, 1989; Fig. 1). The most external of these domains is the Apulia Platform, a ~6 km-thick succession of neritic Mesozoic carbonate rocks (Ricchetti, 1980). This succession is partially overlain by mainly terrigenous marine deposits of Cenozoic age (Patacca and Scandone, 2004; Figs. 1 and 3).

The Apulia Platform and its underlying basement are partly involved in the orogenic wedge (Menardi Noguera and Rea, 2000; Butler et al., 2004), partly form the foreland inflected below the outer front of the Apennines (Mostardini and Merlini, 1986), and partly form the Adriatic foreland *sensu stricto*, both on-land and off-shore (Gargano, Central Apulia, Salento and Southern Adriatic Sea; Fig. 1). Southern Apennines migrated toward the Adriatic foreland up to the beginning of the Middle Pleistocene, when the motion of the wedge front is reported to have ceased (Patacca and Scandone, 2004). Meanwhile, SW-NE–trending extension, already affecting the inner part of the belt (Papanikolaou and Roberts, 2007, among many others), became dominant over the core of the Apennines, probably as a result of a geodynamic change that took place around 800 ka (e.g. Cinque et al., 1993; Hippolyte et al., 1994). This tectonic regime is still active, as demonstrated by breakout and seismicity data (Montone et al., 2004), and accounts for large earthquakes generated by NW-SE–striking normal faults straddling the topographic divide of the Southern Apennines (Gruppo di Lavoro CPTI, 2004; DISS Working Group, 2007, with references; Fig. 2). In contrast, recent instrumental evidence shows that to the northeast of the Apennines ridge the SW-NE extension is associated with NW-SE horizontal compression (Vannucci and Gasperini, 2004; Boncio et al., 2007; Del Gaudio et al., 2005; 2007). For instance, the 2002 Molise earthquakes (Figs. 1 and 2) supplied living evidence that, in the frontal part of the chain, large upper crustal NW-SE normal faults give way to deeper E-W, right-lateral, seismogenic faults (Borre et al., 2003; Di Luccio et al., 2005). Major E-W–oriented shear zones have been described in literature roughly between the latitudes 40°30’N and 42°30’N, both on-land and off-shore (Di Bucci and Mazzoli, 2003; Valensise et al., 2004; both with references). They extend for tens of kilometres below the outer front of the Southern Apennines orogenic wedge and, toward the east, below the foredeep deposits up to the foreland. Their present-day activity is interpreted as due to the reactivation of inherited zones of weakness. Among them, the best constrained is referred to as Molise-Gondola shear zone, that has a clear geologic and seismogenic signature (MGsz; Di Bucci et al., 2006, with references; Fig. 1). Further south, another regional E-W lineament extending between Potenza and Taranto has been recently interpreted as active and seismogenic (DISS Working Group, 2007), as it includes the source area of a series of M5+ earthquakes that were caused by right-lateral slip on E-W planes at 15-23 km depth (1990-1991 Potenza earthquakes; Boncio et al., 2007, with references; Fig. 2).

Assessing whether the southernmost portion of Apulia is tectonically active is made more difficult by the following circumstances: (1) seismicity is low, widespread and seemingly trendless; (2) no information on the active stress field is available from breakout data; (3) geomorphological studies indicate that the southernmost tip of the study area underwent uplift during the Middle Pleistocene, followed by a relative stability during the past 330 ka (Mastronuzzi et al., 2007b), while the Taranto area has been uplifted at 0.14-0.25 mm/a since the Late Pleistocene (Bordoni and Valensise, 1998; Ferranti et al., 2006; Caputo et al., 2007).

*2.2. Quaternary setting*

Although considered as a stable area, the Apulia portion of the Adriatic foreland shows geological evidence for the interplay between the build-up of the Apennines and Dinarides chains and the eustatic sea level changes in Pleistocene times. Therefore, the detailed analysis of the Southern Murge Plateau and Salento Peninsula provides a more complex Quaternary evolution, marked by alternating phases of sea transgression and continentality, that are controlled in part by the tectonic activity.

<u>Bradanic foredeep cycle.</u> During the Late Pliocene-Middle Pleistocene, Apulia was marked by relative sea level stages higher than the present one. During this time interval the foredeep area, submerged by the paleo-Adriatic Sea, was characterized by the deposition of bioclastic calcarenites (Calcareniti di Gravina Fm; e.g., Iannone and Pieri, 1979; D’Alessandro and Iannone, 1982; 1984; Tropeano et al., 2002 and references therein; Fig. 4), giving way to grey-bluish clayey marls toward the Taranto Gulf (Argille subappennine Fm; e.g., Marino, 1996; Ciaranfi et al., 2001; Maiorano et al.,

2008, and references therein). This sedimentary event is closed by coarse terrigenous deposits.

There is partial agreement concerning the interpretation and chronological attribution of the Lower-Middle Pleistocene deposits that crop out in the Salento Peninsula. In this lapse of time, almost the entire Salento was under sub-aerial conditions but its southeasternmost part. Here, bioclastic massive calcarenites heteropic to gray-bluish silty clays have been referred exclusively to the latest Early Pleistocene by Bossio et al. (1991, and references therein). On the contrary, other investigators refer to the Pliocene-Lower Pleistocene stratigraphic interval the deposits which crop out in Salento (Tropeano et al., 2004).

A considerable number of studies is available for the Bradanic foredeep (Ciaranfi et al., 2001; Maiorano et al., 2008 and references therein), whereas very few data have been collected on the silty-clay deposits frequently exposed along the coast between Brindisi and Lecce, or near Taranto (i.e., Ricchetti, 1967; 1972; Fig. 3), at the bottom of the Marine Terraced Deposits (see next subsection). In the former zone, Coppa et al. (2001) dated to the Early-Middle Pleistocene a succession exposed along the Torre San Gennaro cliff. In the latter zone, the age of an ash layer interlayered in the silty clay constrains its deposition at ~1.2 Ma (Capaldi et al., 1979). In the Cheradi Islands, in front of the Taranto harbour, new data from nannoplancton analyses on a silty-sand deposit suggest a Middle Pleistocene age, based on the presence of *Gephyrocapsa* sp3 (Mastronuzzi and Sansò, 1998).

<u>Marine Terraced Deposits.</u> Up to 15-20 m thick, bioclastic, sandy-calcarenitic sediments, the so-called Marine Terraced Deposits, crop out all around the Murge Plateau and in Salento up to an elevation of 300-400 m and are dated Middle-Upper

Pleistocene (Ciaranfi et al., 1988; Fig. 4). Marine sediments are frequently associated with well-cemented aeolian deposits, arranged in a continuous dune belt. These covers formed during repeated marine transgressions, which probably affected only in part, or even never, the eastern and southern part of Salento (Mastronuzzi et al., 2007b).

The best known among the Marine Terraced Deposits are those along the coast stretching from Taranto to Gallipoli, referred to the latest Middle Pleistocene and/or to the Last Interglacial Period (e.g. Hearty and Dai Pra, 1992; Belluomini et al., 2002 and references therein), as well as those belonging to the Middle-Upper Pleistocene succession recognized between Gallipoli and Leuca (D'Alessandro and Massari, 1997). On the contrary, several outcrops in other parts of Salento are still poorly studied.

Middle-Upper Pleistocene deposits can be found also in the inner parts of the study area (D'Alessandro et al., 1994). The complete sedimentary succession, from bottom to top, is formed by massive yellow-greenish clayey sands, very rich in glauconite, called "Sabbie a Brachiopodi" (sands with Brachiopods). The related paleontological assemblage is marked by the presence of *Terebratula scillae* Seguenza and suggests a deposition depth >100 m (D'Alessandro and Palmentola, 1978; D'Alessandro et al., 1994). The Sabbie a Brachiopodi are covered by silty clays of shallower marine environment (Salvatorini 1969; D'Alessandro et al., 1994). An erosional surface separates the top of these deposits from a sandy silt rich in quartz, micas, carbonate rock fragments and scarce oligotypic fauna (mainly *Clamys* sp. and *Ostrea* sp.). Fauna content and sedimentological observations suggest that the sand deposition occurred in shallow waters (Savatorini, 1969), yet below the wave base. In the innermost parts of the study area, these deposits lay directly on the Mesozoic limestone; locally, they shade upward into carbonate-cemented sandstones. An up to 2 m-thick calcareous sandstone (“Panchina”) overlies either the sandy silt or directly the underlying clayey silt through an erosive contact.

Marine Terraced Deposits other than the Sabbie a Brachiopodi are also present in the study area. Along the Ionian side, the two lowermost units are represented by algal biocalcarenites rich in tropical fauna (i.e., *Strombus bubonius* Lamarck, *Cardita calyculata senegalensis* Reeve, *Patella ferruginea* Gmelin, *Hyotissa hyotis* Linnaeus, etc.) and reefal build-ups bio-constructed by *Cladocora caespitosa* Linnaeus. This fossil content, and the impressive set of relative (amino acid racemisation) or absolute (U/Th ratio) age determinations associated, indicates a tropical environment of Late Pleistocene age, that corresponds to the MIS 5.5 (Fig. 4). Deposits referred to sub-stages more recent than MIS 5 are also locally exposed (e.g. Hearthy and Dai Pra, 1992; Belluomini et al., 2002, and references therein).

Along the Adriatic side of the Murge Plateau and of the Brindisi Plain, well-cemented sterile calcarenites with rare bioturbations are exposed, ascribed to a beach/dune environment. The absence of fossil remains did not allow any biostratigraphic correlation or absolute age determination. A rough chronological constraint is provided by a man-splinted flint found in the *colluvium* underlying the beach-dune deposits and ascribed to the Middle Paleolithic-Mousterian Age. This suggests a Late Pleistocene age, corresponding to a generic MIS 5, for the overlying marine deposits (Marsico et al., 2003).

Finally, three generations of dune belts have been referred to the Holocene (Fig. 4). In some places they are associated with beach sediments, which can be recognized along several tracts of the Southern Apulia coast (Mastronuzzi and Sansò, 2002b). The oldest dune generation is the most developed; it is represented by aeolian, poorly cemented, bioclastic sands which retain some *Helix* sp. specimens. A number of radiocarbon age determinations on *Helix* sp., integrated with geomorphological and archaeological data, suggest that these dunes formed about 6.5 ka BP, during the maximum flooding event (Flandrian transgression). The second generation of dune belts, made up of loose brownish sands alternating with soil horizons, formed during the Greek-Roman Age. The last phase of dune formation has been ascribed instead to Medieval times.

<u>Quaternary vertical motions.</u> Within the Quaternary long-term uplift of the Adriatic foreland, which started in the latest Early Pleistocene (Pieri et al., 1996) or during the Middle Pleistocene (Ciaranfi et al., 1983), different landscape units indicate a not homogeneous morphotectonic evolution of the Murge Plateau and Salento Peninsula (Bordoni and Valensise, 1998; Ferranti et al., 2006). This evolution is also accompanied by evidence of pre-, sin- and post-sedimentary tectonic activity, affecting for instance Pleistocene deposits exposed in the surroundings of Bari and Brindisi (Moretti and Tropeano, 1996; Moretti, 2000).

The Murge Plateau is bordered by a staircase of well developed marine erosional/depositional terraces, suggesting that the origin of the plateau is related to the effects of eustatic sea level changes superimposed to long-term regional uplift. On the contrary, the Salento Peninsula, although characterized by a set of horst and graben affecting the Mesozoic bedrock (locally named “Serre”; Palmentola, 1987), displays a flat landscape that makes more complex to read the interplay between uplift and eustatism. The Sabbie a Brachiopodi sedimentation has been related to a marked subsidence occurred at least in the western and inner parts of Salento during the Middle Pleistocene (D’Alessandro et al., 1994). A subsequent uplift was then responsible for the emersion of wide sectors of the peninsula. The uplift-rate strongly decreased at MIS

9.3, about 330 ka BP (Mastronuzzi et al., 2007b); since then, maximum values of uplift-rate have been recorded only in the Taranto area (0.25 mm/a; Ferranti et al., 2006), whereas they taper to zero in the southernmost part of the region (Dai Pra and Hearthy 1988; Hearthy and Dai Pra, 1992; Belluomini et al., 2002). Finally, a slow subsidence seems to characterize at present the Adriatic side of the Apulia region (Mastronuzzi and Sansò, 2002c; Marsico et al., 2003; Lambeck et al., 2004).

## 3. Mesostructural analysis

### *3.1. Methodological approach*

This paper deals with brittle fractures characterized by a displacement vector with a prevailing component orthogonal to the fracture surface and a negligible shear component. These tectonic features are here referred to as “extension joints” and are mainly associated with a mode-I propagation mechanism (e.g. Hancock, 1985; Pollard and Aydin, 1988; Engelder, 1994). Only extension joints have been considered in our statistical analyses, that we carried out by applying an inversion technique proposed by Caputo and Caputo (1989) in order to infer the orientation of the principal stress axes and their ratio. The basic assumptions for the application of this numerical method are (i) that two orthogonal joint sets within the same site be genetically related to a unique remote causative stress field, and (ii) that they both consist of pure extension joints. Both assumptions must be verified directly in the field by checking intersection geometries and displacement vectors. In case (i), we observe mutual abutting relationships documenting geologically coeval joint sets, therefore associated with the same remote stress field. In case (ii), we observe that the displacement vectors are systematically at high angle, almost perpendicular to the fracture planes, documenting the opening mode-I and therefore the tensile origin of the joints.

The mechanical model is based on the principle that, given a single joint, the principal minimum stress axis $\sigma_3$ is perpendicular to the fracture plane while the maximum principal stress axis $\sigma_1$ is parallel to it, though with a not determined direction. In case of two coeval orthogonal joints, it is possible to determine the orientation of the $\sigma_1$, which is parallel to the intersection between the planes. When a statistically significant number of joints cluster in two roughly orthogonal sets, an inversion technique can be applied to infer the orientation of the principal stress axes. Coarsely speaking, the "mean" direction of all intersections represents the $\sigma_1$, while the barycenters of the poles to the planes of the two sets represent the remote principal stress axes $\sigma_2$ and $\sigma_3$. The $\sigma_3$ axis corresponds to the denser cluster of poles (i.e., to the most developed extension joint set). To avoid bias from data collection, we spent an effort to carefully seek 3D outcrops. The use of a least square method and of a Lagrange multiplier assures that the three mean directions are mutually orthogonal as theoretically expected (Caputo and Caputo, 1989).

In reality, the fact that two mutually abutting orthogonal joint sets affect a rock mass implies that the stress field has continuously varied during the brittle deformational phase. In particular, as far as the $\sigma_3$ is always perpendicular to an extensional joint during its formation, it must have been alternatively oriented in the two directions defined by the two joint sets and inferred by the numerical method. This local variation is explained by a "swap mechanism" caused by the stress release associated with, and intrinsic to, the fracturing process (Caputo, 1995; 2005). As a consequence, although the remote $\sigma_2$ and $\sigma_3$ are stable in time, when a rock volume undergoes extensional fracturing, the local $\sigma_2$ and $\sigma_3$ axes temporarily swap, interchanging repeatedly their orientation. Finally, the proposed inversion technique also allows us to calculate the ratio R = $(\sigma_2 - \sigma_3)/(\sigma_1 - \sigma_3)$, which is an important parameter indicative of the shape of the mean stress ellipsoid.

The proposed methodological approach shows a limitation when applied to sites where only one joint set occurs with an associated R $\cong$ 1. In these cases, we cannot rule out the hypothesis that $\sigma_1 \neq \sigma_2$, because it is also possible that $\sigma_1$ and $\sigma_2$ absolute values did not allow the inception of the stress swap mechanism. Accordingly, the stress tensor could be triaxial and, in principle, correspond to either a normal Andersonian regime ($\sigma_z = \sigma_1$) or a transcurrent one ($\sigma_z = \sigma_2$).

### *3.2. Paleostresses from extensional joints analysis*

In order to get information about the Middle-Late Quaternary tectonic evolution of the study region, we investigated numerous sites by measuring the joint orientations and their opening vectors. Observations have been made both on sub-horizontal surfaces and on two or more vertical sections views, thus attempting a 3D vision of the outcrops, which were often represented by quarries (Figs. 4 and 5). In particular, the analysis of the quarry floors allowed a correct interpretation of the number and organization of the orthogonal joint sets measured along the walls, avoiding to undersample one of the two sets. To guarantee statistically reliable results of the quantitative analyses, for each site we measured as many joints as possible, ensuring a minimum of 20-30 fractures per joint system. Particular care was spent in the field to check the possible occurrence (indeed never detected) of horizontal extensional joints. Figure 6 shows some examples of the analyzed joint systems, where fractures are plotted as poles to the planes in stereographic projections (lower hemisphere). The principal stress axes, $\sigma_1$, $\sigma_2$ and $\sigma_3$, are represented as triangles, rhombi and squares, respectively. The size of the symbols is proportional to the amount of opening and length of the joints, as measured in the field. This information has been included in the numerical inversions as a statistical weight because, when dealing with extensional veins, both cumulative opening and total length are somehow proportional to the number of fracturing events occurred and hence to the remote tensile conditions.

Similar to most inversion techniques used in mesostructural analyses (Carey and Brunier, 1974; Angelier, 1975; Etchecopar et al., 1981; Armijo et al., 1982; Reches, 1987; Caputo and Caputo, 1988; Huang, 1989), also the method applied in this paper (Caputo and Caputo, 1989) follows the assumption that the amount of displacement (in our case, of opening) associated with the fracture system is negligible with respect to the dimensions of the investigated rock volume. If such assumption must be carefully verified in the field when analyzing faults, it is obvious for the sites considered in this work, which are affected only by extension joints. As an often implicit consequence of this general assumption, the calculated strain tensor can be considered co-axial with the causative stress tensor and hence a kinematic information like the amount of opening can be safely used as a statistical weight. A further reason for using opening and joint length in the numerical inversion follows the observation that large and thick veins are commonly the result of several rupture events (Caputo and Hancock, 1999). We do not consider joint spacing (or density) because it mainly depends on the distribution of subsequent fracturing events (e.g. crack-seal versus crack-jump mechanisms) and not on the remote tensile stress.

In the numerous sites investigated, the extension joints form sets of nearly parallel planes. Locally a unique joint set was recognized (Fig. 6a), but the occurrence of two well developed, roughly orthogonal sets is more common (Fig. 6b). In few but crucial cases, more than two joint sets exist (Fig. 6c and d).

Following the basic concepts proposed by Hancock (1985) to determine the relative timing of fractures, in the field we spent particular care to observe the occurrence of mutual or systematic abutting relationships between joints belonging to different sets (Fig. 5). Accordingly, we considered the corresponding joint sets as geologically coeval or not, respectively. In the former case, the two joint sets have been analyzed as a unique joint system, while in the latter case the two sets have been separated before performing the numerical inversions (Fig. 6c and d).

## 4. Discussion

Based on the mesostructural analysis of the Quaternary deposits cropping out in Salento and on the numerical inversions of the acquired datasets, our results suggest some immediate simple considerations. Firstly, all the "local" stress tensors calculated for each site are characterized by a vertical maximum principal stress axis ($\sigma_1$), therefore documenting the occurrence of an extensional tectonic regime (*sensu* Anderson, 1942) throughout the entire area. Secondly, the two horizontal principal stress axes ($\sigma_2$ and $\sigma_3$), although variably oriented in the different sites, show some recurrent directions. Thirdly, in some sites we observed two distinct joint systems, that we interpret as the result of different stress fields occurred in subsequent periods. These considerations are developed in the following.

### *4.1. Tectonic stratigraphy*

The "tectonic stratigraphy" of an area is defined as the structural evolution that can be reconstructed for that zone by determining (i) the number of deformational events occurred in a given time interval, (ii) the related stress trajectories or the average stress field, (iii) the areal distribution of the associated deformation structures, i.e., the dimensions of the crustal volume involved, and (iv) in case of two or more events, their relative and absolute chronology (Caputo and Pavlides, 1993).

In this perspective, we can reconstruct the Middle and Late Quaternary tectonic stratigraphy of the southern Adriatic foreland of Italy, as all the studied sites have been selected exclusively in carbonate deposits not older than the late Lower Pleistocene. This choice allows a detailed chronology of the most recent deformational events, although it implies a scattered distribution of the sites suitable for the structural analysis.

By integrating such analysis of the extension joints with geological and litho-stratigraphic information, we were able to organize our dataset in three subsets of data. For each subset, the corresponding mesostructural analysis returned fairly uniform results, indicating the occurrence of at least three separate deformational events during the Middle and Late Quaternary. These three subsets are shown separately in Tables 1 to 3 (from the oldest to the most recent deformational event, respectively) and in the corresponding Figure 7a, b and c. We will discuss each subset individually.

In the tables, the occurrence within the same site of two distinct joint systems is also emphasized in the column "*relative age*". In this case, the relative chronology is also indicated, as evaluated in the field. Moreover, on the right-hand columns, for each site we reported the directions of the three principal stress axes and the stress ratio R.

The first subset of data includes six sites with horizontal $\sigma_2$ and $\sigma_3$ roughly trending N-S and/or E-W (Tab. 1). These localities are distributed all over the investigated area (Fig. 7a), therefore suggesting the regional significance of this deformational event. In many cases, the E-W joint set dominates, while locally the N-S prevails (e.g. Sal034, where, however, local effects cannot be ruled out). In all cases, extension is almost uniaxial, as documented by the ratio R that varies in the 0.64-0.99 interval, with prevailing values near the upper bound. Abutting relationships with the other joints analyzed show that the joint sets belonging to this first subset of data are constantly older than the other ones. Moreover, they were never observed in rocks younger than the late Lower Pleistocene. Taking into account the age of the hosting deposits and the age of the second subset of data (see below in this same section), the deformational event represented by the first subset of data is constrained to the early and middle part of the Middle Pleistocene.

The stress variability observed within this subset could be tentatively explained in different ways. Firstly, it could be artificial, i.e., we grouped not coeval stress fields. However, the relatively tight chronological constraint does not favour this hypothesis, that would assume the occurrence of more than one deformational event in a very short time window. Secondly, as far as all the measured stress fields are representative of very superficial crustal rocks, they were characterized by low magnitude stresses. Therefore, they could have been very sensitive to local effects due, for example, to underlying inherited structures, lithological variations or morphological irregularities. However, the relatively limited number of investigated sites does not help to definitely confirm this explanation. Thirdly, as above discussed, when $R \cong 1$ and only one joint set occurs (as in the cases of sites Sal061 and Sal067; Fig. 7a), the possibility that the stress tensor be triaxial and the tectonic regime purely tensional ($\sigma_z = \sigma_1$) or transcurrent ($\sigma_z = \sigma_2$) cannot be ruled out.

The second subset of data has been observed in ten sites (Fig. 7b and Tab. 2). The estimated stress tensors are characterized by an almost uniaxial tension, represented by an ellipsoid of revolution around the horizontal $\sigma_3$ axis. The orientation of the least principal stress ranges between N22° and N62°, with a mean value of ~N43° (Fig. 8). The stress ratio R is high, ranging between 0.85 and 0.99. Also in this case, due to method limitations, the occurrence of sites with only one joint set (e.g. Sal066 and Sal069; Fig. 7b) explains the local misorientation of the $\sigma_1$ and $\sigma_2$ axes, that could be part of a triaxial tensor. This NE-SW extension characterizes the Early-Middle Pleistocene rocks whereas it was never observed in Late Quaternary deposits. Based on sites characterized by more than one joint system (e.g. site Sal072), this event is clearly older than the deformational event associated with the third subset of data, while it is younger than the joint system belonging to the first subset of data (Sal012 and Sal064). Therefore, a late Middle Pleistocene age can be reasonably assigned to this deformational event.

The third subset of data includes twelve sites covering the entire investigated area (Fig. 7c and Tab. 3). The common feature which characterizes the sites of this subset is a low R ratio, with values that never exceed 0.47 and are frequently lower than 0.30. Such values correspond to an ellipsoid that tends to be of revolution around the $\sigma_1$ vertical axis; the $\sigma_2$ and $\sigma_3$ axes are comparable, thus indicating a sort of horizontal 'radial' extension. Even though the remote $\sigma_2$ and $\sigma_3$ axes were quite similar in magnitude, at least as a space and time average, due to the stress swap mechanism the related joints commonly cluster in two roughly orthogonal sets statistically equivalent.

All the youngest investigated sites, consisting of Upper Pleistocene calcarenites, are included in this subset, whereas sites characterized by older Quaternary deposits show systematic abutting relationships. Accordingly, this deformational event is not older than the Late Pleistocene and possibly reflects the active stress field still pervading (at least) the shallower sectors of the entire study area.

We consider unlikely the hypothesis of this event as resulting from the superposition of local conditions on a regional stress field analogous to that associated to the second event. Beyond the difference in age of the affected deposits, many of the sites coincide in the two subsets, and this rules out possible local causes at the outcrop scale. Moreover, the wide distribution of the third subset of data all over the study area can be better explained by a large scale cause.

*4.2. Geodynamic perspective*

From a seismotectonic point of view, the documented mild deformation, joined with the lack of major, active, emergent faults (e.g. like the Mattinata fault in the Gargano Promontory; Fig. 1) and with the scarce historical and instrumental seismicity (Fig. 2), do not favour the hypothesis of large seismogenic sources in the study area, whereas the occurrence of moderate earthquakes cannot be ruled out. Moreover, with regard to the recent geodynamics of the southern Adriatic foreland, we observe that, within a general extension, during the Middle and Late Pleistocene our study area underwent second order yet detectable variations of the principal stress axes with time intervals in the order of few hundred ka. Comparable variations affecting the southern Adriatic foreland during the Middle and Late Quaternary have been already suggested for a sector north of our study area, the Gondola fault zone in the Gargano off-shore (Fig. 1). In this zone, Ridente and Trincardi (2006) and Ridente et al. (2008) infer analogous intensity variations of the tectonic activity along the fault zone, and recognize a relative maximum of deformation in the latest Middle Pleistocene (230-250 to 130-140 ka), followed by a still evident yet less intense tectonic activity. This independent result confirms what suggested by our data, i.e., the recent tectonic evolution of the southern

Adriatic foreland is marked by weak deformation whose intensity varies through time sufficiently to determine surface evidence of this variation.

The oldest deformational event found (Fig. 8a) is referred to the early and middle part of the Middle Pleistocene. As mentioned in the previous sections, in the same time interval the Southern Apennines were just undergoing a geodynamic change characterized by (i) the inception of a SW-NE extension over the chain ridge, (ii) the end of the east-northeastward motion of the wedge front in the Bradanic foredeep, and (iii) the beginning of a long-term uplift in the Apulia region. The oldest deformational event could be thus interpreted as the response of the foreland to the contractional regime responsible for the last motion of the Southern Apennines front (Patacca and Scandone, 2004; Fig. 1).

The penultimate deformational event is referred to the latest Middle Pleistocene and is characterized by a SW-NE extension accompanied by high R values (Fig. 8b). This extension is widespread and characterised by well organized and defined pattern of planes, with limited dispersion with respect to the dominant direction. From a regional perspective, a SW-NE extension is not surprising. For instance, NW-SE graben structures involving Plio-Quaternary deposits off-shore, southeast of Salento, have already been described by Argnani et al. (2001). The same investigators interpret this deformation as an outer-arc extension due to the flexure of the Adriatic foreland.

Different causes have been proposed in the literature for this flexure, showing that the debate on the geodynamics of the Adriatic block is indeed a lively one, but also that for this tectonic domain the Middle and Late Quaternary geodynamic evolution has always been considered as a whole, without more detailed analyses. For instance:

1. Billi and Salvini (2003) consider the flexure of Apulia as the on-shore forebulge of the Adriatic foreland, and interpret in this perspective of flexural processes the NW-SE systematic joints measured in the Mesozoic carbonate rocks.
2. Various investigators invoke the buckling of a thick continental lithosphere as a possible cause, either within an active subduction beneath the Southern Apennines (Doglioni et al., 1994) or due to horizontal compression, also associated with the Albanides convergence (Bertotti et al., 2001).
3. Moreover, although most researchers set the end of Southern Apennines thrusting around the beginning of the Middle Pleistocene (e.g. Butler et al., 2004; Patacca and Scandone, 2004), others contend that at that time thrusting did not cease and possibly shifted to the northeast, progressively involving the Adriatic “foreland” (Caputo and Bianca, 2005; Ferranti and Oldow, 2006; Caputo et al., 2007). Within this latter scenario, SW-NE extension could be explained as the result of a crustal-scale extrados stretching, that is to say, as the surface evidence of a deep ramp anticline associated with a thrust detachment rooting within the crystalline part of the Adriatic crust.
4. Besides, the Salento and its off-shore counterpart form the flexural bulge of the eastern, lateral portion of the Calabrian arc (Doglioni et al., 1999), that is an orogenic wedge associated with a subducting slab of oceanic lithosphere (Faccenna et al., 2003, with references). The recent SW-NE extension of our study area could also be related to this deeper engine.
5. Finally, since the Late Tortonian the general geodynamic frame of the Adriatic foreland is dominated by the Africa motion toward stable Europe along NNW-SSE to NW-SE vectors (e.g. Mazzoli and Helman, 1994). The SW-NE extension of the study area could also be interpreted as a consequence of this convergence.

Summarizing, all these geodynamic models justify a SW-NE active extension in the study area. On the one hand, our data confirm this extension and supply new chronological constraints for its activity; on the other hand, they obviously cannot provide the key to define a preferred geodynamic model.

All these models can be also compared with the most recent deformational event described in this work (Fig. 8c), characterized by low R ratio and by a horizontal, almost radial extension (*viz.* comparable $\sigma_2$ and $\sigma_3$), emphasized by the high angular deviation of $\sigma_2$ and $\sigma_3$ (±54° in both cases, with 18° overlap, therefore totally interchangeable from a statistical point of view). If we compare this sort of "doming" of the study area with the previous deformational event, we have to hypothesize a Late Pleistocene stress field variation which encompasses a relative decrease of the $\sigma_2$ with respect to the $\sigma_3$ (or increase of the $\sigma_3$ with respect to the $\sigma_2$). This kind of evolution and the final doming observed suggest a geodynamic setting where two orthogonal engines compete (Fig. 9).

The ongoing slab subduction beneath the Calabrian arc is outlined by seismicity data (Giardini and Velonà, 1991; Castello et al., 2005), and the related wedge front deforms the seafloor in the Ionian Sea (Doglioni et al., 1999). In the Taranto Gulf, the Calabrian wedge is in structural continuity with the Southern Apennines wedge (Bigi et al., 1990; Figs. 2 and 9). Tilted Upper Pleistocene marine deposits suggest a possible weak activity also for the latter wedge (Caputo et al., 2007). This activity should taper to zero moving towards the NW, where according to Patacca and Scandone (2004) the migration of the Southern Apennines toward the Adriatic foreland ceased at the beginning of the Middle Pleistocene (~650 ka). Along the northeastern side of the Adriatic Sea, the compressional regime presently affecting the Dinarides, Albanides and the northern Hellenides fold-and-thrust belts is well depicted by the relevant seismicity and related focal mechanisms (Harvard CMT Project 2006). Finally, the current geodynamic frame of the Adriatic foreland is still dominated by the NW-SE Eurasia-Nubia convergence (Serpelloni et al., 2007; Devoti et al., 2008; Fig. 9). This convergence has been interpreted as responsible for the active deformation of other parts of the Adriatic foreland (e.g. the MSsz; Di Bucci and Mazzoli, 2003; Valensise et al., 2004; Di Bucci et al., 2006; Ridente et al., 2008) and it is compatible with the seismicity recorded on-land in different parts of the southern Adriatic foreland, both exposed and inflected below the outer front of the southern Apennines (Borre et al., 2003; Di Luccio et al., 2005; Del Gaudio et al., 2005; 2007; Boncio et al., 2007).

On these bases, the two engines hypothesized could be tentatively found on the one hand in the Calabrian arc (in particular its lateral portion in the Taranto Gulf) and Dinarides-Albanides-Hellenides chain, and on the other hand in the NW-SE Eurasia-Nubia convergence (Fig. 9). Together, they could provide the competing horizontal forces needed to determine the observed doming and the consequent fibre stresses (e.g. Argnani et al., 2001; Billi and Salvini, 2003).

## 5. Final remarks

The method applied in this work to study orthogonal extensional joints turns out to be suitable for the analysis of the recent-to-active stress field in foreland areas affected by mild deformation. The southern Adriatic foreland of Italy has a crucial location in the Central Mediterranean tectonic domains. Therefore, the identification of the recent (-to-active) stress field of this region, mild but not negligible as considered up to now, can provide a key to interpret the relationships among these tectonic domains. For the Middle and -at least- Late Pleistocene, our results suggest an overall homogeneous framework of shallow (upper crustal) extension, with three deformational events of regional significance that can be recognized within this general extensional regime.

The oldest event, constrained to the early and middle part of the Middle Pleistocene, is characterized by variable direction of extension. The penultimate event, dated late Middle Pleistocene, is characterized by an almost uniaxial tension, with a horizontal $\sigma_3$ striking SW-NE. The most recent event is characterized by a horizontal 'radial' extension; it is not older than the Late Pleistocene and possibly reflects the active stress field still dominating the entire study area. The deformation associated with this stress field can be described as a sort of doming, and it has been tentatively explained as the result of two geodynamic far-ranging components that act simultaneously: (i) the Calabrian arc and the Dinarides-Albanides-Hellenides chain, and (ii) the NW-SE Eurasia-Nubia convergence. Together, they could provide the competing horizontal stresses needed to determine the observed doming of this crustal i.e. rigid block.

## Acknowledgments

Thanks are due to P. Boncio, D. Peacock, G. Roberts and G. Valensise for criticisms and fruitful discussions. The work benefited from the constructive review by J. Galindo-Zaldivar, A.M. Michetti and the Editor L. Piccardi, who are kindly acknowledged. Study supported by the Project S2 funded in the framework of the 2004-2006 agreement between the Italian Department of Civil Protection and the INGV (Research Units 2.4-Burrato, 2.11-Mastronuzzi). Scientific papers funded by DPC do not represent its official opinion and policies.

## References

Anderson, E.M., 1942. The dynamics of faulting and dyke formation with applications to Britain. Oliver and Boyd, 191 pp., Edinburgh.

Angelier, J., 1975. Sur un apport de l'informatique à l'analyse structurale: exemple de la tectonique cassante. Revue de Géographie Physique et de Géologie Dynamique 17 (2), 137-146.

Argnani, A., Rugosi, F., Cosi, R., Ligi, M., Favali, P., 2001. Tectonics and seismicity of the Apulian Ridge south of Salento peninsula (Southern Italy). Annals of Geophysics 44, 527-540.

Armijo, R., Carey, E., Cisternas, A., 1982. The inverse problem in microtectonics and the separation of tectonic phases. Tectonophysics 82, 145-160.

Belluomini, G., Caldara, M., Casini, C., Cerasoli, M., Manfra, L., Mastronuzzi, G., Palmentola, G., Sansò, P., Tuccimei, P., Vesica, P.L., 2002. The age of Late Pleistocene shorelines and tectonic activity of Taranto area, Southern Italy. Quaternary Science Reviews 21, 525-547.

Bertotti, G., Picotti, V., Chilovi, C., Fantoni, R., Merlini, S., Mosconi, A., 2001. Neogene to Quaternary sedimentary basins in the south Adriatic (Central Mediterranean): foredeeps and lithospheric buckling. Tectonics 20 (5), 771-787.

Bigi, G., Cosentino, D., Parotto, M., Sartori, R., Scandone, P., 1990. Structural Model of Italy and Gravity Map. CNR, P.F. Geodinamica, Quaderni de "La ricerca scientifica" 114, 3, six sheets.

Billi, A., Salvini, F., 2003. Development of systematic joints in response to flexure related fibre stress in flexed foreland plates: the Apulian forebulge case history, Italy. Journal of Geodynamics 36, 523-536.

Boncio, P., Mancini, T., Lavecchia, G., Selvaggi, G., 2007, Seismotectonics of strike-slip earthquakes within the deep crust of southern Italy: geometry, kinematics, stress field and crustal reology of the Potenza 1990-1991 seismic sequences. Tectonophysics, doi: 10.1016/j.tecto.2007.08.016.

Bordoni, P., Valensise, G., 1998. Deformation of the 125 ks marine terrace in Italy: tectonic implications. In: Stewart, I.S., Vita Finzi, C. (Eds.), Coastal Tectonics. Geological Society, London, Special Publications 146, 71-110.

Borre, K., Cacon, S., Cello, G., Kontny, B., Kostak, B., Likke Andersen, H., Moratti, G., Piccardi, L., Stemberk, J., Tondi, E., Vilimek, V., 2003, The COST project in Italy: analysis and monitoring of seismogenic faults in the Gargano and Norcia areas (central-southern Apennines, Italy). Journal of Geodynamics 36, 3-18.

Bossio, A., Mazzei, R., Monteforti, B., Salvatorini, G., 1991. Note geologiche e stratigrafiche sull'area di Palmariggi (Lecce, Puglia). Rivista Italiana di Paleontologia Stratigrafica 97 (2), 175-234.

Butler, R.W.H., Mazzoli, S., Corrado, S., De Donatis, M., Scrocca, D., Di Bucci, D., Gambini, R., Naso, G., Nicolai, C., Shiner, P., Zucconi, V., 2004. Applying thick-skinned tectonic models to the Apennine thrust belt of Italy - Limitations and implications: In: McClay, K. (Ed.), Thrust tectonics and hydrocarbon systems. American Association of Petroleum Geologists Memoir 82, 647-667.

Capaldi, G., Civetta, L., Lirer, L., Munno, R., 1979. Caratteri Petrografici ed età K/Ar delle cineriti intercalate nelleformazioni argillose pleistoceniche della Fossa Bradanica. Geologia Applicata ed Idrogeologia 14 (3), 493-501.

Caputo, M., Caputo, R., 1988. Structural analysis: new analytical approach and applications. Annales Tectonicae 2 (2), 84-89.

Caputo, M., Caputo, R., 1989. Estimate of the regional stress field using joint systems. Bulletin of the Geological Society of Greece 23 (1), 101-118.

Caputo, R., 1995. Evolution of orthogonal sets of coeval extension joints. Terra Nova 7 (4), 479-490.

Caputo, R., 2005. Stress variability and brittle tectonic structures. Earth-Science Reviews 70 (1-2), 103-127.

Caputo, R., Bianca, M., 2005. Morphological evidence of Late Quaternary thrusting in the Bradanic Foredeep. Rend. Soc. Geol. It., 1, nuova serie, 75-76.

Caputo, R., Hancock, P.L., 1999. Crack-jump mechanism of microvein formation and its implications for stress cyclicity during extension fracturing. Journal of Geodynamics 27, 45-60.

Caputo, R., Pavlides, S., 1993. Late Cainozoic geodynamic evolution of Thessaly and surroundings (Central-Northern Greece). Tectonophysics 223 (3-4), 339-362.

Caputo, R., Bianca, M., D'Onofrio, R., 2007. Is the orogenic activity still active in the external Southern Apennines?. 6th Forum GeoItalia, Rimini, September 11-15, 2007. Epitome 2, 236.

Carey, E., Brunier, B., 1974. Analyse théorique et numérique d'un modèle mécanique élémentaire appliqué à l'étude d'une population de failles. Comptes rendus de l'Académie des Sciences de Paris D279, 891-894.

Castello, B., Selvaggi, G., Chiarabba, C., Amato, A., 2005. CSI, Catalogo della sismicità italiana 1981-2002, versione 1.0. INGV-CNT, Roma. http://www.ingv.it/CSI/

Ciaranfi, N., Ghisetti, F., Guida, M., Iaccarino, G., Lambiase S., Pieri, P., Rapisardi, L., Ricchetti, G., Torre, M., Tortorici, L., Vezzani, L., 1983. Carta Neotettonica dell'Italia Meridionale. CNR, P.F. Geodinamica 515, 1-62.

Ciaranfi, N., Pieri, P., Ricchetti, G., 1988. Note alla carta geologica delle Murge e del Salento (Puglia centromeridionale), 1:250.000. Memorie della Società Geologica Italiana 42, 449-460.

Ciaranfi, N., Pasini, G., Rio, D., 2001. The meeting on the Plio-Pleistocene boundary and the Lower/Middle Pleistocene transition: type areas and sections (Bari, 25-29 September 2000). Memorie di Scienze Geologiche 53, 1-123.

Cinque, A., Patacca, E., Scandone, P., Tozzi, M., 1993. Quaternary kinematic evolution of the southern Apennines. Relationship between surface geological features and deep lithospheric structures. Annali di Geofisica 36, 249-260.

Console, R., Di Giovambattista, R., Favali, P., Presgrave, B.W., Smriglio, G., 1993. Seismicity of the Adriatic microplate. Tectonophysics 218, 343-354.

Coppa, M.G., De Castro, P., Marino, M., Rosso, A., Sanfilippo, R., 2001. The Pleistocene with Aequipecten opercularis (Linneo) of “Campo di Mare” (Brindisi, Italy). Bollettino della Società Paleontologica Italiana 40 (3), 405-429.

D'Alessandro, A., Iannone, A., 1982. Pleistocene carbonate deposits in the area of Monopoli (Bari Province): sedimentology and palaeocology. Geologica Romana 21, 603-653.

D'Alessandro, A., Iannone, A., 1984. Prime considerazioni sedimentologiche e paleoecologiche su alcune sezioni della Calcarenite di Gravina (Pleistocene) nei pressi di Monopoli. Studi di Geologia e Geofisica 27, 1-16.

D'Alessandro, A., Massari, F., 1997. Pliocene and Pleistocene depositional environments in the Pesculuse area (Salento, Italy). Rivista Italiana di Paleontologia e Stratigrafia 103, 221-258.

D'Alessandro, A., Palmentola, G., 1978. Sabbie e Brachiopodi, una nuova unità del Salento leccese (aspetti litosfratigraflci e paleoambientali). Rivista Italiana di Paleontologia e Stratigrafia 84, 1083-1120.

D'Alessandro, A., Mastronuzzi, G., Palmentola, G., Sansò, P., 1994. Pleistocene deposits of Salento leccese (Southern Italy): problematic relationships. Bollettino della Società Paleontologica Italiana 33 (2), 257-263.

Dai Pra, G., and Hearty, P.J., 1988. I livelli marini pleistocenici del Golfo di Taranto, sintesi geocronostratigrafica e tettonica. Memorie della Società Geologica Italiana 41, 637-644.

Del Gaudio, V., Pierri, P., Calcagnile, G., Venisti, N., 2005, Characteristics of the low energy seismicity of central Apulia (southern Italy) and hazard implications. Journal of Seismology 9, 39-59.

Del Gaudio, V., Pierri, P., Frepoli, A., Calcagnile, G., Venisti, N., Cimini, G.B., 2007. A critical revision of the seismicity of Northern Apulia (Adriatic microplate - Southern Italy) and implications for the identification of seismogenic structures. Tectonophysics 436, 9-35.

Devoti, D., Riguzzi, F., Cuffaro, M., Doglioni, C., 2008. New GPS constraints on the kinematics of the Apennines subduction. Earth Planet. Sci. Lett. 273, 163-174.

Di Bucci, D., Mazzoli, S., 2003. The October-November 2002 Molise seismic sequence (southern Italy): an expression of Adria intraplate deformation. Journal of the Geological Society London 160, 503-506.

Di Bucci, D., Ravaglia, A., Seno, S., Toscani, G., Fracassi, U., Valensise, G., 2006. Seismotectonics of the Southern Apennines and Adriatic foreland: insights on active regional E-W shear zones from analogue modelling. Tectonics 25, TC4015, doi: 10.1029/2005TC001898.

Di Bucci, D., Coccia, S., Fracassi, U., Iurilli, V., Mastronuzzi, G., Palmentola, G., Sansò, P., Selleri, G., Valensise, G., 2009a. Late Quaternary deformation of the southern Adriatic foreland (southern Apulia) from mesostructural data: preliminary results. Bollettino della Società Geologica Italiana (Italian Journal of Geosciences) 128 (1), 33-46.

Di Bucci, D., Ridente, D., Fracassi, U., Trincardi, F., Valensise, G., 2009b. Marine paleoseismology from Very High Resolution seismic imaging: the Gondola Fault

Zone (Adriatic foreland). Terra Nova 21 (5), 393-400. doi: 10.1111/j.1365-3121.2009.00895.x

Di Luccio, F., Fukuyama, E., Pino, N.A., 2005. The 2002 Molise earthquake sequenze: what can we learn about the tectonics of southern Italy?. Tectonophysics 405, 141-154.

DISS Working Group, 2007. Database of Individual Seismogenic Sources (DISS), Version 3.0.4: A compilation of potential sources for earthquakes larger than M 5.5 in Italy and surrounding areas. http://www.ingv.it/DISS/, © INGV 2005, 2007. All rights reserved.

Doglioni, C., Mongelli, F., Pieri, P., 1994. The Puglia uplift (SE-Italy): an anomaly in the foreland of the Apenninic subduction due to buckling of a thick continental lithosphere. Tectonics 13, 1309-1321.

Doglioni, C., Merlini, S., Cantarella, G., 1999. Foredeep geometries at the front of the Apennines in the Ionian Sea (central Mediterranean). Earth and Planetary Science Letters 168, 243-254.

Engelder, T., 1994. Brittle crack propagation. In: Hancock, P.L. (Ed.), Continental Deformation. Pergamon Press, Oxford, 43-52.

Etchecopar, A., Vasseur, G., Daignieres, M., 1981. An inverse problem in microtectonics for the determination of stress tensors from fault striation analysis. Journal of Structural Geology 3 (1), 51-65.

Faccenna, C., Jolivet, L., Piromallo, C., Morelli, A., 2003. Subduction and the depth of convection in the Mediterranean mantle. Journal of Geophysical Research 108 (B2), 2099, doi:10.1029/2001JB001690.

Ferranti, L., Oldow, J.S., 2006. Rates of late Neogene deformation along the southwestern margin of Adria, southern Apennines orogen, Italy, *in* Pinter, N., et al., eds., The Adria Microplate: GPS Geodesy, Tectonics, and Hazards. Springer, NATO Science Series IV, 61, 109-131.

Ferranti, L., Antonioli, F., Mauz, B., Amorosi, A., Dai Pra, G., Mastronuzzi, G., Monaco, C., Orrù, P., Pappalardo, M., Radtke, U., Renda, P., Romano, P., Sansò, P., Verrubbi, V., 2006. Markers of the last interglacial sea-level high stand along the coast of Italy: Tectonic implications. Quaternary International 145-146, 30-54.

Fracassi, U., Valensise, G., 2007. Unveiling the sources of the catastrophic 1456 multiple earthquake: Hints to an unexplored tectonic mechanism in Southern Italy. Bulletin of the Seismological Society of America 97 (3), 725-748.

Funiciello, R., Montone, P., Parotto, M., Salvini, F., Tozzi, M., 1991. Geodynamical evolution of an intra-orogenic foreland: the Apulia case history (Italy). Bollettino della Società Geologica Italiana 110, 419-425.

Giardini, D., Velonà, M., 1991. Deep seismicity of the Tyrrhenian Sea. Terra Nova 3, 57-64.

Gruppo di Lavoro CPTI, 2004. Catalogo Parametrico dei Terremoti Italiani, vers. 2004 (CPTI04). INGV, Bologna, http://emidius.mi.ingv.it/CPTI/

Guidoboni, E., Ferrari, G. 2004. Revisione e integrazione di ricerca riguardante il massimo terremoto storico della Puglia: 20 febbraio 1743. RPT 272A/05, SGA – Storia Geofisica Ambiente, Bologna, 103 pp.

Hancock, P.L., 1985. Brittle microtectonics: principles and practice. Journal of Structural Geology 7 (3-4), 437-457.

Harvard University, 2006. Harvard Centroid-Moment Tensor Project. http://www.seismology.harvard.edu/projects/CMT/

Hearty, P.J., Dai Pra, G., 1992. The age and stratigraphy of Quaternary coastal deposits along the gulf of Taranto (south Italy). Journal of Coastal Research 8 (4), 882-905.

Hippolyte, J.-C., Angelier, J., Roure, F., 1994. A major geodynamic change revealed by Quaternary stress patterns in the Southern Apennines (Italy). Tectonophysics 230, 199-210.

Huang, Q., 1989. Modal and vectorial analysis for determination of stress axes associated with fault slip data. Mathematical Geology 21 (5), 543-558.

Iannone, A., Pieri, P., 1979. Considerazioni critiche sui “Tufi calcarei” delle Murge. Nuovi datii litostratigrafici e paleoambientali. Geografia Fisica e Dinamica Quaternaria 2, 173-186.

Lambeck, K., Anzidei, M., Antonioli, F., Benini, A., Esposito, E., 2004. Sea level in Roman time in the Central Mediterranean and implications for modern sea level rise. Earth and Planetary Science Letters 224, 563-575.

Maiorano, P., Aiello, G., Barra, D, Di Leo, P., Joannin, S., Lirer, F., Marino, M., Pappalardo, A., Capotondi, L., Ciaranfi, N., Stefanelli, S., 2008. Paleoenvironmental changes during sapropel 19 (i-cycle 90) deposition: Evidences from geochemical, mineralogical and micropaleontological proxies in the mid-Pleistocene Montalbano Jonico land section (southern Italy). Palaeogeography, Palaeoclimatology, Palaeoecology 257(3), 308-334. doi: 10.1016/j.palaeo.2007.10.025S0031-0182(07)00543-3.

Marino, M., 1996. Quantitative calcareous nannofossil biostratigraphy of the Lower-Middle Pleistocene, Montalbano Jonico section (Southern Italy). Palaeopelagos 6, 347-360.

Marsico, A., Selleri, A., Mastronuzzi, G., Sansò, P., Walsh, N., 2003. Cryptokarst: a case-study of the Quaternary landforms of southern Apulia (southern Italy). Acta Carsologica 32 (2), 147-159.

Mastronuzzi, G., Sansò, P., 1998. Morfologia e genesi delle Isole Chéradi e del Mar Grande (Taranto, Puglia, Italia). Geografia Fisica e Dinamica Quaternaria 21, 131-138.

Mastronuzzi, G., Sansò, P., 2000. Boulders transport by catastrophic waves along the Ionian coast of Apulia (southern Italy). Marine Geology 170, 93-103.

Mastronuzzi, G., Sansò, P., 2002a. Holocene uplift rates and historical rapid sea-level changes at the Gargano promontory, Italy. Journal of Quaternary Science 17 (5-6), 593-606.

Mastronuzzi, G., Sansò, P., 2002b. Holocene coastal dune development and environmental changes in Apulia (Southern Italy). Sedimentary Geology 150, 139-152.

Mastronuzzi, G., Sansò, P., 2002c. Pleistocene sea level changes, sapping processes and development of valleys network in Apulia region (southern Italy). Geomorphology 46, 19-34.

Mastronuzzi, G., Sansò, P., 2004. Large boulder accumulation by extreme waves along the Adriatic coast of southern Apulia (Italy). Quaternary International 120, 173-184.

Mastronuzzi, G., Pignatelli, C., Sansò, P., Selleri, G., 2007a. Boulder accumulations produced by the 20th February 1743 tsunami along the coast of southeastern Salento (Apulia region, Italy). Marine Geology 242 (1-3), 191-205, doi:10.1016/j.margeo.2006.10.025.

Mastronuzzi, G., Quinif, Y., Sansò, P., Selleri, G., 2007b. Middle-Late Pleistocene polycyclic evolution of a geologically stable coastal area (southern Apulia, Italy). Geomorphology 86, 393-408.

Mazzoli, S., Helman M., 1994, Neogene patterns of relative plate motion for Africa–Europe: Some implications for recent central Mediterranean tectonics. Geologische Rundschau 83, 464-468.

Menardi Noguera, A., Rea, G., 2000. Deep structure of the Campanian-Lucanian Arc (southern Apennines). Tectonophysics 324, 239-265.

Montone, P., Mariucci, M.T., Pondrelli, S., Amato, A., 2004. An improved stress map for Italy and surrounding regions (central Mediterranean). Journal of Geophysical Research 109, B10410, 1-22, doi: 10.1029/1003JB002703.

Moretti, M., 2000. Soft-sediment deformation structures interpreted as seismites in middle-late Pleistocene aeolian deposits (Apulian foreland, Southern Italy). Sedimentology 135, 167-179.

Moretti, M., Tropeano, M., 1996. Strutture sedimentarie deformative (sismiti) nei depositi tirreniani di Bari. Memorie della Società Geologica Italiana 51, 485-500.

Mostardini, F., Merlini, S., 1986. Appennino centro-meridionale. Sezioni Geologiche e Proposta di Modello Strutturale. Memorie della Società Geologica Italiana 35, 177-202.

Palmentola, G., 1987. Lineamenti geologici e morfologici del Salento leccese. Atti del "Convegno sulle conoscenze geologiche del territorio salentino". Quaderni di Ricerca del Centro Studi di Geotecnica e d'Ingegneria 11, 173-202.

Papanikolaou, I.D., Roberts, G.P., 2007. Geometry, kinematics and deformation rates along the active normal fault system in the southern Apennines: Implications for fault growth. Journal of Structural Geology 29, 166-188.

Patacca, E., Scandone, P., 1989. Post-Tortonian mountain building in the Apennines. The role of the passive sinking of a relic lithospheric slab. In: Boriani, A.M., et al. (Eds.), The Lithosphere in Italy. Atti dei Convegni Lincei 80, 157-176.

Patacca, E., Scandone, P., 2004. The Plio-Pleistocene thrust belt – foredeep system in the Southern Apennines and Sicily (Italy). In: Crescenti, U., et al. (Eds.), Geology of Italy. Società Geologica Italiana, Roma, 93-129.

Piccardi, L., 2005. Paleoseismic evidence of legendary earthquakes: the apparition of Archangel Michael at Monte Sant'Angelo (Italy). Tectonophysics 408, 113-128.

Pieri, P., Sabato, L., Tropeano, M., 1996. Significato Geodinamico dei caratteri deposizionali e strutturali della Fossa Bradanica nel Pleistocene. Memorie della Società Geologica Italiana 51, 501-515.

Pollard, D.D., Aydin, A., 1988. Progress in understanding jointing over the past century. Bulletin of the Geological Society of America 100, 1181-1204.

Reches, Z., 1987. Determination of the tectonic stress tensor from slip along faults that obey the Coulomb yield condition. Tectonophysics 6 (6), 849-861.

Ricchetti, G., 1967. Osservazioni preliminari sulla geologia e morfologia dei depositi quaternari nei dintorni del Mar Piccolo (Taranto). Atti Accademia Gioenia Scienze Naturali in Catania 6 (18), 123-130.

Ricchetti, G., 1972. Osservazioni geologiche e morfologiche preliminari sui depositi quaternari affioranti nel F. 203 (Brindisi). Bollettino della Società dei Naturalisti in Napoli 81, 543-566.

Ricchetti, G., 1980. Contributo alla conoscenza strutturale della Fossa Bradanica e delle Murge. Bollettino della Società Geologica Italiana 99, 421-430.

Ridente, D., Trincardi, F., 2006. Active foreland deformation evidenced by shallow folds and faults affecting late Quaternary shelf-slope deposits (Adriatic Sea, Italy). Basin Research 18 (2), 171-188. doi: 10.1111/j.1365-2117.2006.00289.x

Ridente, D., Fracassi, U., Di Bucci, D., Trincardi, F., Valensise, G., 2008. Middle Pleistocene to Holocene activity of the Gondola Fault Zone (Southern Adriatic Foreland): deformation of a regional shear zone and seismotectonic implications. In: Caputo, R., Pavlides, S. (Eds.), Earthquake Geology: methods and applications. Tectonophysics 453 (1-4), 110-121. doi:10.1016/j.tecto.2007.05.009

Salvatorini, G., 1969. Contributo alla conoscenza delle microfaune pleistoceniche della penisola salentina. Atti della Società Toscana di Scienze Naturali 76 (1), 232-260.

Serpelloni, E., Vannucci, G., Pondrelli, S., Argnani, A., Casula, G., Anzidei, M., Baldi, P., Gasperini, P., 2007. Kinematics of the Western Africa-Eurasia plate boundary from focal mechanisms and GPS data. Geophysical Journal International (Online-Early Articles). doi:10.1111/j.1365-246X.2007.03367.x

Servizio Geologico d'Italia, 1967. Carta Geologica d'Italia, Fogli: 202 Taranto, 203 Brindisi, 204 Lecce, 213 Maruggio, 214 Gallipoli, 215 Otranto, 223 Capo S. Maria di Leuca, 1:100.000. Servizio Geologico d'Italia, Roma.

Tinti, S., Maramai, A., Graziani, L., 2004. The new catalogue of Italian tsunamis. Natural Hazards 33, 439-465.

Tropeano, M., Pieri, P., Moretti, M., Festa, V., Calcagnile, G., Del Gaudio, V., Pierri, P. 1997. Tettonica quaternaria ed elementi di sismotettonica nell'area delle Murge (Avampaese Apulo). Il Quaternario 10 (2), 543-548.

Tropeano, M., Sabato, L., Pieri, P., 2002. Filling and cannibalization of a foredeep: the Bradanic Trough (Southern Italy). In: Jones, S.J., Frostick, L.E. (Eds.), Sediment flux to basins: causes, controls and consequences. Geological Society of London Sp. Publ. 191, 55-79.

Tropeano, M., Spalluto, L., Moretti, M., Pieri, P., Sabato, L., 2004. Depositi carbonatici infrapleistocenici di tipo Foramol in sistemi di scarpata (Salento, Ialia

Meridionale). Il Quaternario, Italian Journal of Quaternary Sciences 17 (2-2), 537-546.

Valensise, G., Pantosti, D., Basili, R., 2004. Seismology and Tectonic Setting of the Molise Earthquake Sequence of October 31-November 1, 2002. Earthquake Spectra 20, 23-37.

Vannucci, G., Gasperini, P., 2004. The new release of the database of Earthquake Mechanisms of the Mediterranean Area (EMMA Version 2). Annals of Geophysics Suppl. 47, 307-334.

**Figure captions**

**Fig. 1.**
Geological sketch map of Southern Italy (Calabrian arc excluded). The Molise-Gondola shear zone (MGsz) is also shown.

**Fig. 2.**
Historical and instrumental earthquakes of the Central and Southern Apennines (M>4.0; Gruppo di lavoro CPTI, 2004; Vannucci and Gasperini, 2004; Harvard CMT Project, 2006; Fracassi and Valensise, 2007). The size of the square symbols is proportional to an equivalent magnitude derived from intensity data. The black thick line is the outer front of the Southern Apennines buried below the foredeep deposits.

**Fig. 3.**
Geological sketch of the Salento Peninsula (redrawn, data from sources mentioned in the legend). The Apulia carbonate platform (of Cretaceous-Paleocene age) crops out primarily in the topographic highs to the N and NW (the Murge Plateau) and toward the SE sector of Salento. Lower to Upper Pleistocene deposits are exposed in the Brindisi Plain, along the coast from Porto Cesareo to Taranto and S of Gallipoli. Pleistocene to Holocene deposits can be found only in few localities, mostly on the western sector of the studied area but for the Otranto surroundings. Pl-Ho: Pleistocene-Holocene alluvium; MUPl: Middle-Upper Pleistocene terraced coastal plain and limestone breccias; MiPl: Middle Pleistocene sands (Sabbie di Montemarano Fm); LoPl: Lower Pleistocene shales and marls (Argille subappennine Fm) and calcarenites and littoral calcirudites (Calcareniti di Gravina Fm); K-LT: Lower Tertiary open shelf carbonates (Pietra Leccese and Calcareniti di Andrano Fms) and Cretaceous platform limestone (Calcare di Bari and Calcare di Altamura Fms). Simplified from Ciaranfi et al. (1988).

**Fig. 4.**
Examples of analyzed deposits: **a**) cemented dune, Holocene, site Sal009 (Lon. E 17.701, Lat. N 40.760), **b**) marine calcarenites with *Strombus bubonius* Linnaeus, Upper Pleistocene, site Sal033, **c**) Marine Terraced Deposits, Middle-Upper Pleistocene, site Sal032; **d**) Gravina Fm marine calcarenites, late Lower Pleistocene, site Sal019.

**Fig. 5.**

Examples of analyzed joints: **a**) extension joints at the outcrop scale, site Sal021; **b**) systematic joint set, site Sal069; **c**) orthogonal joint sets, site Sal011; **d**) two joints chronologically distinguished, i.e., an older calcite-filled fracture cut by a younger sedimentary vein, site Sal034.

**Fig. 6.**

Examples of analysis of the joint systems, where fractures are plotted as poles to the planes in stereographic projections, lower hemisphere. The size of the symbols (crosses) is proportional to the corresponding amount of opening and length of the joints. The latter information has been included in the numerical inversions as a statistical weight. Triangles, rhombi and squares represent the principal stress axes $\sigma_1$, $\sigma_2$ and $\sigma_3$, respectively. Referring to these axes, the upper triplets of numbers indicate azimuth and plunge, while the lower ones represent the normalized weight from which the ratio R is obtained. **a**) Single joint set. **b**) Two well developed, roughly orthogonal sets. **c**) and **d**) More than two joint sets within the same site (black and gray crosses). In these latter cases, data have been separated before applying the numerical inversion method (Caputo and Caputo 1989). See text for further details.

**Fig. 7.**

Deformational events recognized. For each plot, the number on the top-right refers to the site label (see also Tabs. 1 to 3). On the maps, the arrows in the large circles show the direction of horizontal extension, while the gray-scale of the circles refers to the age of the youngest deposit involved at the site (black = late Lower Pleistocene; gray = Middle, late Middle and Middle-Upper Pleistocene; white = Upper Pleistocene). The small white dots are all the investigated sites. **a**) First subset of data (see also Tab. 1), that has been associated with the oldest deformational event recognized, ascribed to the early and middle part of the Middle Pleistocene. **b**) Second subset of data (see also Tab. 2), that has been associated with the penultimate deformational event defined, ascribed to the late Middle Pleistocene. **c**) Third subset of data (see also Tab. 3), that has been associated with the most recent deformational event recognized, not older than the Late Pleistocene.

**Fig. 8.**

Summary of the deformational events defined. Each plot shows the principal axes grouped per event, and their mean values (larger symbols; angular deviation in parentheses). Events are referred to the: **a**) early and middle part of the Middle Pleistocene (site Sal034 omitted); **b**) late Middle Pleistocene; **c**) Late Pleistocene. See also Figures 7a-c and Tables 1-3.

**Fig. 9.**

Geodynamic interpretation proposed in this work. Dashed lines are depth contours in kilometres of the subducting slab. A gray line marks the axis of the Apennine-Maghrebian chain, that is currently undergoing extension. The Africa plate relative motion, referred to the Europe fixed reference (thick black arrows), is from Devoti et al. (2008). Large gray arrows indicate the front motion of the schematised chains.

## Table captions

**Table 1.**

First subset of data collected within the investigated area (see also Fig. 7a). Data refer to the oldest deformational event recognized, ascribed to the early and middle part of the Middle Pleistocene. The *age* is that of the youngest deposits involved at the site. The *relative age* indicates the occurrence of abutting relationships with a joint system associated with another deformational event. The latter subset of data is represented in the corresponding table only if a statistically meaningful numerical inversion has been performed. $\sigma_1$, $\sigma_2$ and $\sigma_3$ are the principal stress axes (maximum, intermediate and minimum, respectively). *R* is the stress ratio: $(\sigma_2 - \sigma_3)/(\sigma_1 - \sigma_3)$.

**Table 2.**

Second subset of data collected within the investigated area (see also Fig. 7b). Data refer to the penultimate deformational event recognized, ascribed to the late Middle Pleistocene. Explanations as in Table 1.

**Table 3.**

Third subset of data collected within the investigated area (see also Fig. 7c). Data refer to the most recent deformational event recognized, not older than the Late Pleistocene. Explanations as in Table 1.

**Table 1.** *First subset of data.*

| *label* | *long. (°E)* | *lat. (°N)* | *location* | *lithology / formation* | *age* | *relative age* | *# of data* | *σ1 azim/dip* | *σ2 azim/dip* | *σ3 azim/dip* | *R* |
|---|---|---|---|---|---|---|---|---|---|---|---|
| Sal012 | 17.192 | 41.012 | Torre Incina | Marine calcarenite (Gravina Fm) | late Early Pleistocene | older than subset 2 | 54 | 119/88 | 282/02 | 012/01 | 0.87 |
| Sal034 | 18.449 | 40.029 | Torre di Porto Miggiano | Marine calcarenite (Gravina Fm) | late Early Pleistocene | possibly older than subset 1 | 105 | 146/83 | 001/06 | 271/04 | 0.98 |
| Sal061 | 17.739 | 40.341 | Avetrana quarry | Marine calcarenite (Gravina Fm) | late Early Pleistocene | | 66 | 285/85 | 098/05 | 188/01 | 0.99 |
| Sal063 | 18.394 | 39.861 | Novaglie | Marine calcarenite (Gravina Fm) | late Early Pleistocene | | 74 | 046/86 | 267/03 | 177/03 | 0.64 |
| Sal064 | 18.137 | 40.334 | Lecce by-pass road (Monteroni) | Marine calcarenite (Gravina Fm) | late Early Pleistocene | older than subset 2 | 134 | 090/88 | 282/02 | 192/00 | 0.97 |
| Sal067 | 17.669 | 40.477 | Oria quarry | Marine calcarenite (Gravina Fm) | late Early Pleistocene | | 101 | 102/41 | 276/49 | 009/03 | 0.99 |

**Table 2.** *Second subset of data.*

| label | long. (°E) | lat. (°N) | location | lithology / formation | age | relative age | # of data | σ1 azim/dip | σ2 azim/dip | σ3 azim/dip | R |
|---|---|---|---|---|---|---|---|---|---|---|---|
| Sal012 | 17.192 | 41.012 | Torre Incina | Marine calcarenite (Gravina Fm) | late Early Pleistocene | older than subset 3 | 33 | 348/82 | 151/08 | 242/02 | 0.98 |
| Sal022 | 18.122 | 40.498 | Casalabate, Intendenza di Finanza | Marine calcarenite with quartz | Middle Pleistocene | | 30 | 145/89 | 303/01 | 033/00 | 0.90 |
| Sal032 | 18.027 | 40.057 | Gallipoli. S. Maria delle Grazie quarry | Terraced marine calcarenite | late Middle Pleistocene | younger than subset 1 | 20 | 129/82 | 322/07 | 232/02 | 0.91 |
| Sal064 | 18.137 | 40.334 | Lecce by-pass road (Monteroni) | Marine calcarenite (Gravina Fm) | late Early Pleistocene | older than subset 3 | 21 | 134/28 | 329/62 | 227/06 | 0.99 |
| Sal065 | 17.794 | 40.441 | W of San Pancrazio Salentino | Marine calcarenite (Gravina Fm) | late Early Pleistocene | | 22 | 084/84 | 321/03 | 231/05 | 0.99 |
| Sal066 | 17.807 | 40.453 | S. Antonio | Marine calcarenite (Gravina Fm) | late Early Pleistocene | | 36 | 038/89 | 131/00 | 221/01 | 0.95 |
| Sal069 | 18.044 | 40.156 | Castellino, quarry between Nardò and Galatone | Marine calcarenite (Gravina Fm) | late Early Pleistocene | | 151 | 148/21 | 330/69 | 238/01 | 0.99 |
| Sal070 | 18.103 | 40.073 | Tuglie quarry | Marine calcarenite (Gravina Fm) | late Early Pleistocene | | 25 | 274/87 | 112/03 | 022/01 | 0.85 |
| Sal072 | 18.115 | 40.506 | Torre Specchiolla, N of Casalabate | Terraced marine deposits, clinostratified | Middle-Late Pleistocene | younger than subset 1 | 53 | 336/90 | 122/00 | 212/00 | 0.90 |
| Sal077 | 17.912 | 40.267 | Porto Cesareo, Crossroad Nardò-Avetrana | Marine calcarenite (Gravina Fm) | late Early Pleistocene | | 103 | 044/87 | 307/00 | 217/03 | 0.86 |

**Table 3.** *Third subset of data.*

| ***label*** | ***long. (°E)*** | ***lat. (°N)*** | ***location*** | ***lithology / formation*** | ***age*** | ***relative age*** | ***# of data*** | ***σ1 azim/dip*** | ***σ2 azim/dip*** | ***σ3 azim/dip*** | ***R*** |
|---|---|---|---|---|---|---|---|---|---|---|---|
| Sal011 | 17.192 | 41.015 | S. Vito Abbey | Marine calcarenite (Gravina Fm) | late Early Pleistocene | | 115 | 255/89 | 072/01 | 162/00 | 0.20 |
| Sal021 | 17.936 | 40.683 | Punta Penne | Clinostratified calcarenite, split (drift NW to SE) | Late Pleistocene? | | 74 | 314/87 | 182/02 | 092/02 | 0.22 |
| Sal032 | 18.027 | 40.057 | Gallipoli. S. Maria delle Grazie quarry | Terraced marine calcarenite | late Middle Pleistocene | younger than subset 2 | 31 | 121/87 | 287/03 | 017/01 | 0.47 |
| Sal033 | 17.993 | 40.061 | Gallipoli coast | Marine calcarenite with *Strombus bubonius* | Late Pleistocene | | 25 | 253/88 | 029/02 | 119/02 | 0.42 |
| Sal034 | 18.449 | 40.029 | Torre di Porto Miggiano | Marine calcarenite (Gravina Fm) | late Early Pleistocene | younger than subset 1 | 57 | 085/86 | 178/00 | 268/04 | 0.14 |
| Sal059 | 17.642 | 40.776 | Costa Merlata | Marine calcarenite (Gravina Fm) | late Early Pleistocene | | 61 | 207/89 | 031/00 | 301/00 | 0.30 |
| Sal062 | 18.408 | 39.976 | Andrano, Grottaverde | Marine calcarenite (Gravina Fm) | late Early Pleistocene | | 32 | 276/88 | 099/02 | 009/00 | 0.16 |
| Sal071 | 18.112 | 40.494 | Quarry near Casalabate | Terraced marine deposits | Middle-Late Pleistocene | | 51 | 086/88 | 298/01 | 208/01 | 0.47 |
| Sal072 | 18.115 | 40.506 | Torre Specchiolla, N of Casalabate | Terraced marine deposits; clinostratified | Middle-Late Pleistocene | younger than subset 2 | 42 | 162/89 | 351/01 | 261/00 | 0.47 |
| Sal074-Sal075 | 18.093 | 39.897 | N of Torre S. Giovanni and Isola dei Pazzi | Dune with foresets and bioturbations Dune overlying marine calcarenite rich in algae | Late Pleistocene | | 24 | 137/88 | 029/01 | 299/02 | 0.17 |
| Sal076 | 18.111 | 39.886 | S of Torre S. Giovanni | Marine calcarenite rich in algae | Late Pleistocene | | 54 | 013/89 | 171/00 | 261/00 | 0.04 |
| Sal078 | 17.358 | 40.354 | Lido Silvana, Pulsano | Calcarenite | Late Pleistocene | | 26 | 034/83 | 278/03 | 187/06 | 0.45 |

Figure 1
Click here to download high resolution image

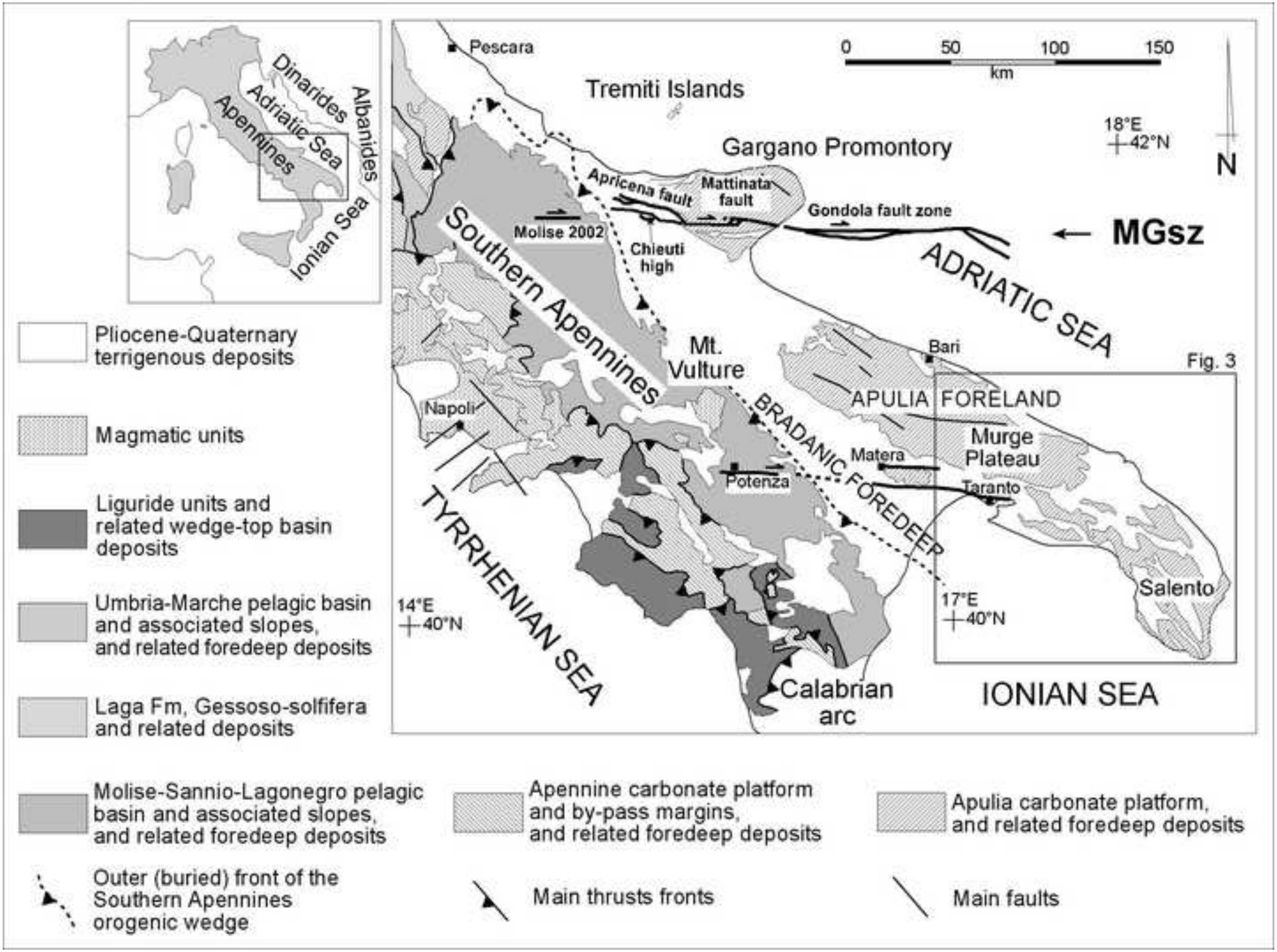

Figure 2

Click here to download high resolution image

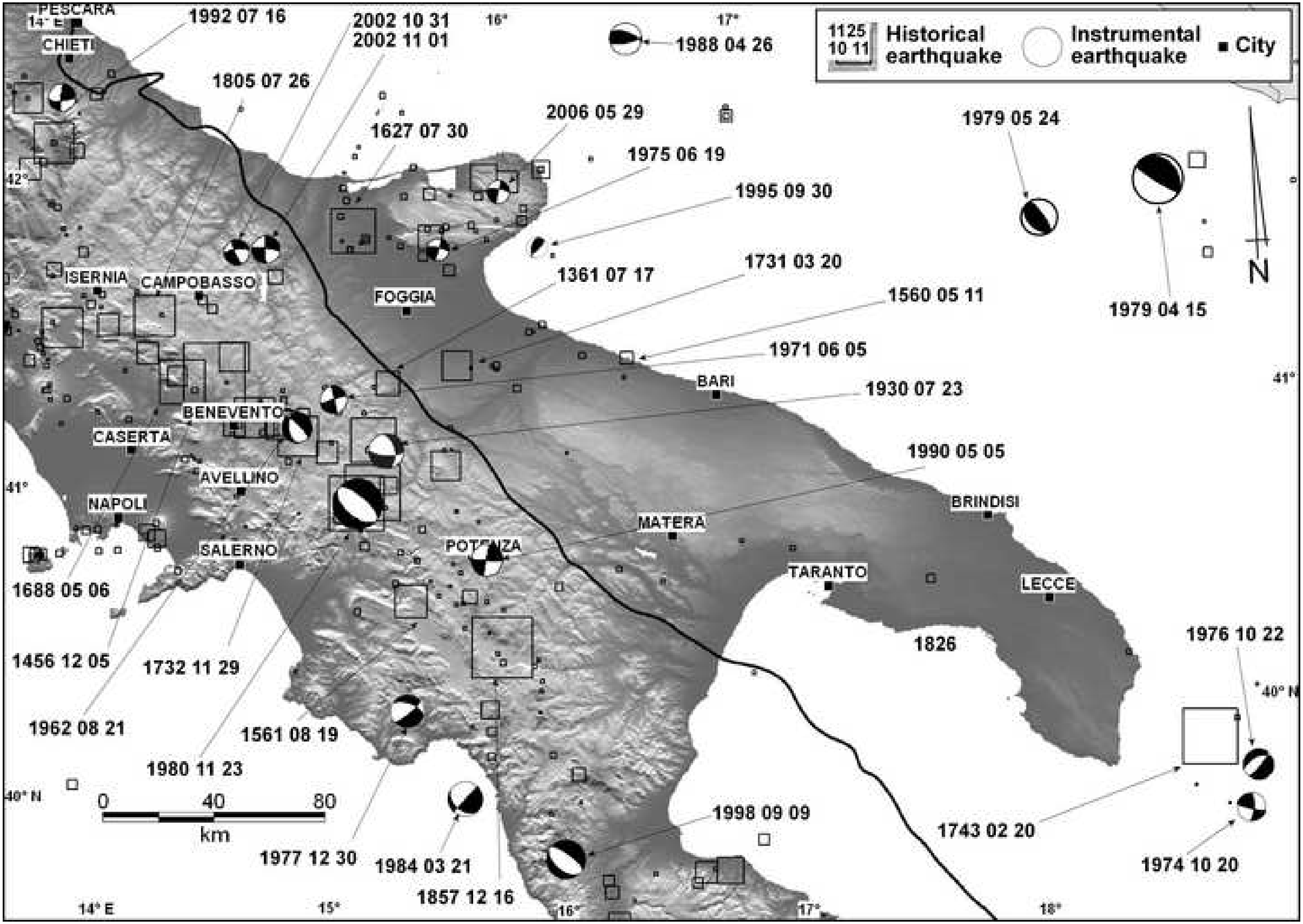

Figure 3

Click here to download high resolution image

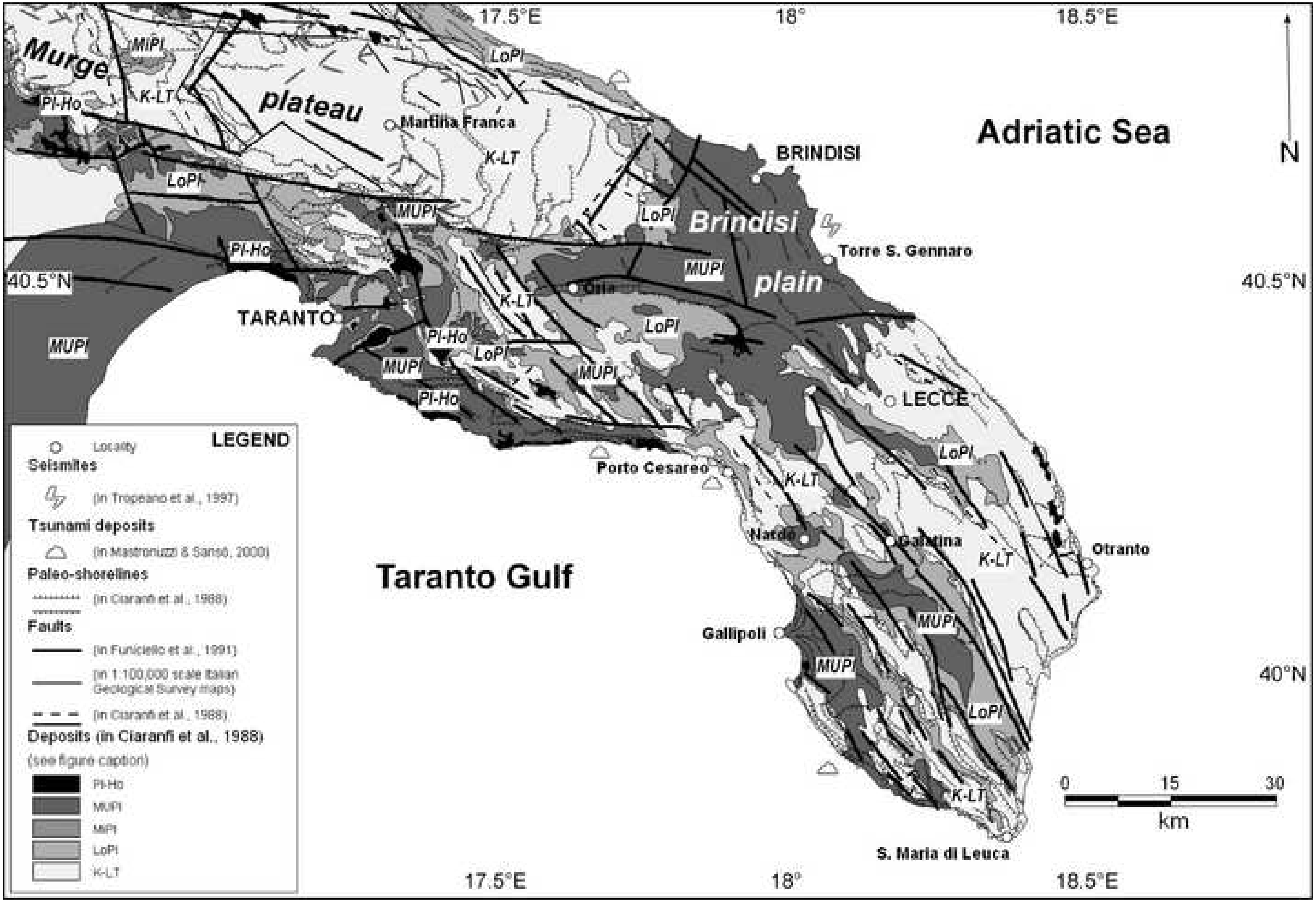

Figure 4
Click here to download high resolution image

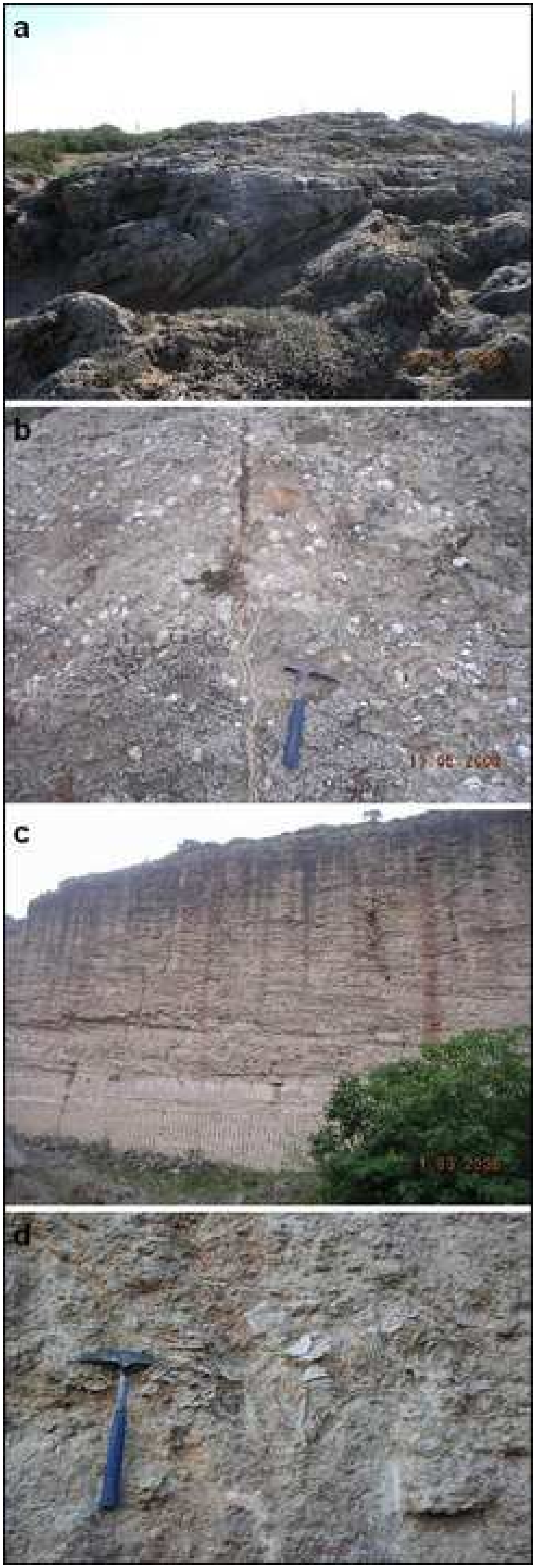

Figure 5
Click here to download high resolution image

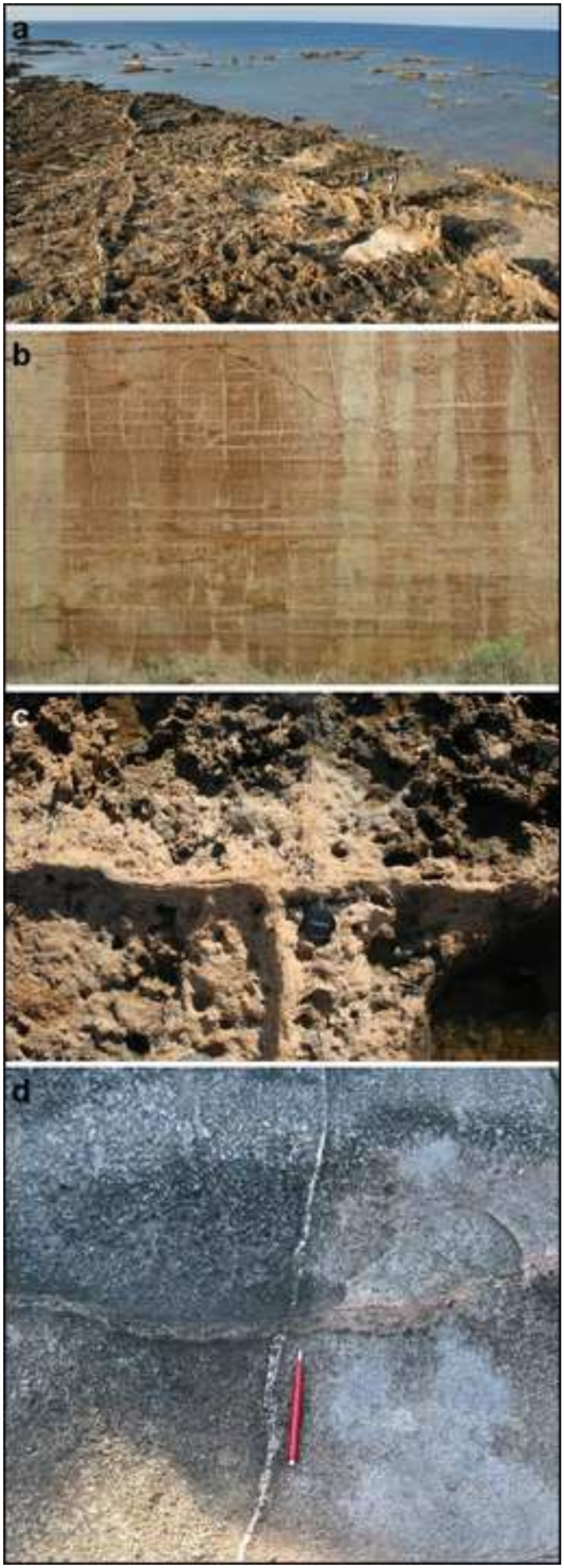

Figure 6
Click here to download high resolution image

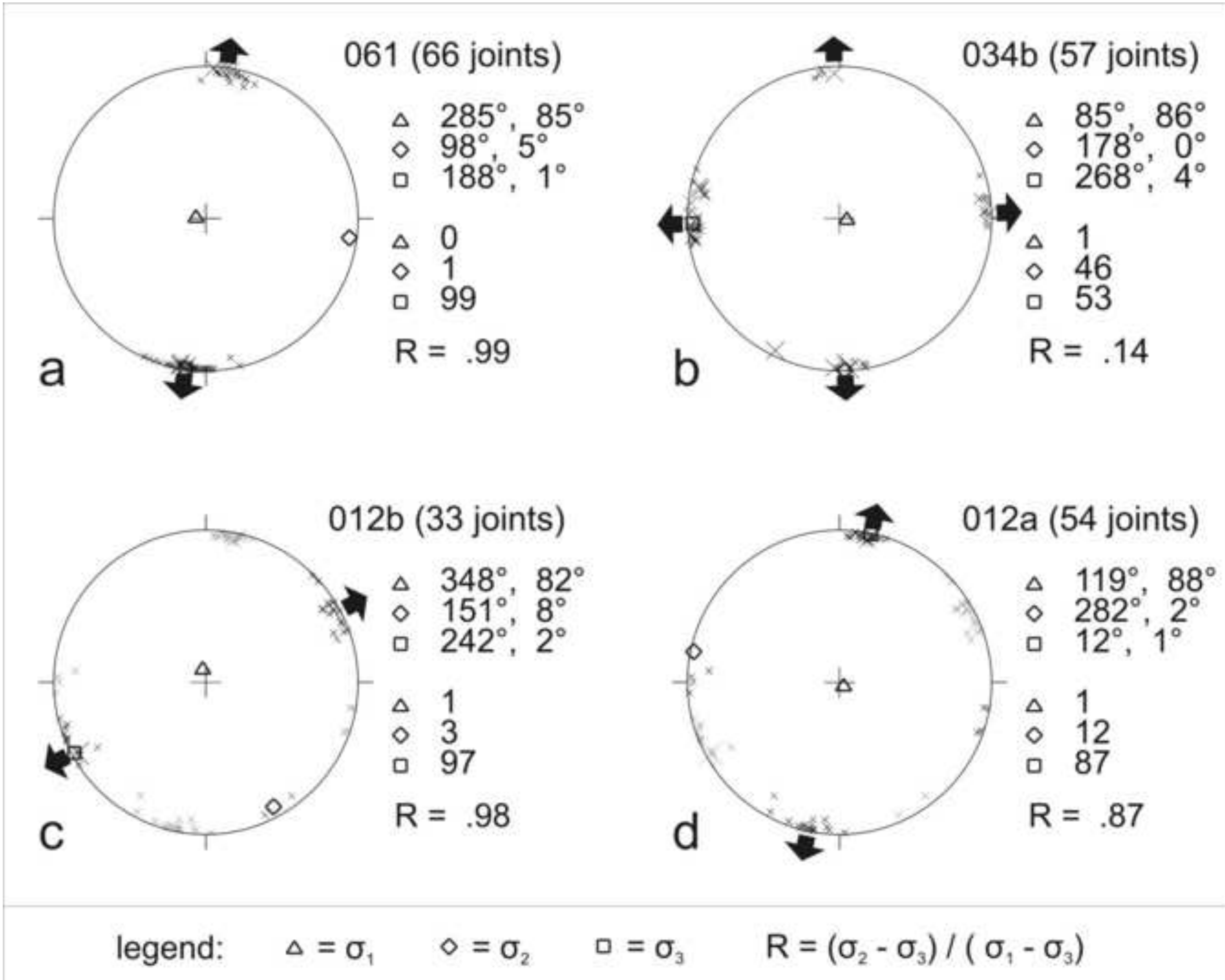

Figure 7a
Click here to download high resolution image

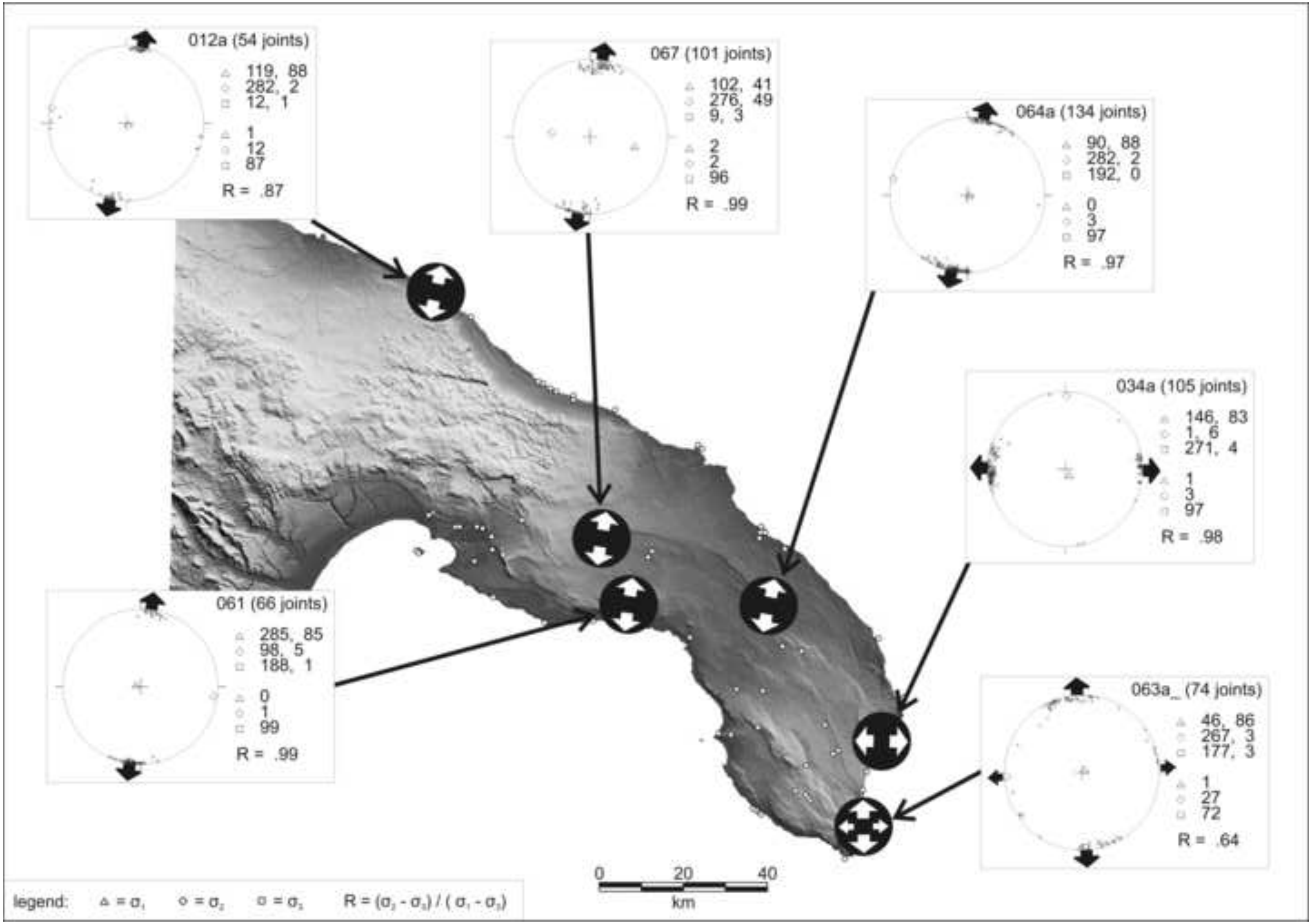

**Figure 7b**

Click here to download high resolution image

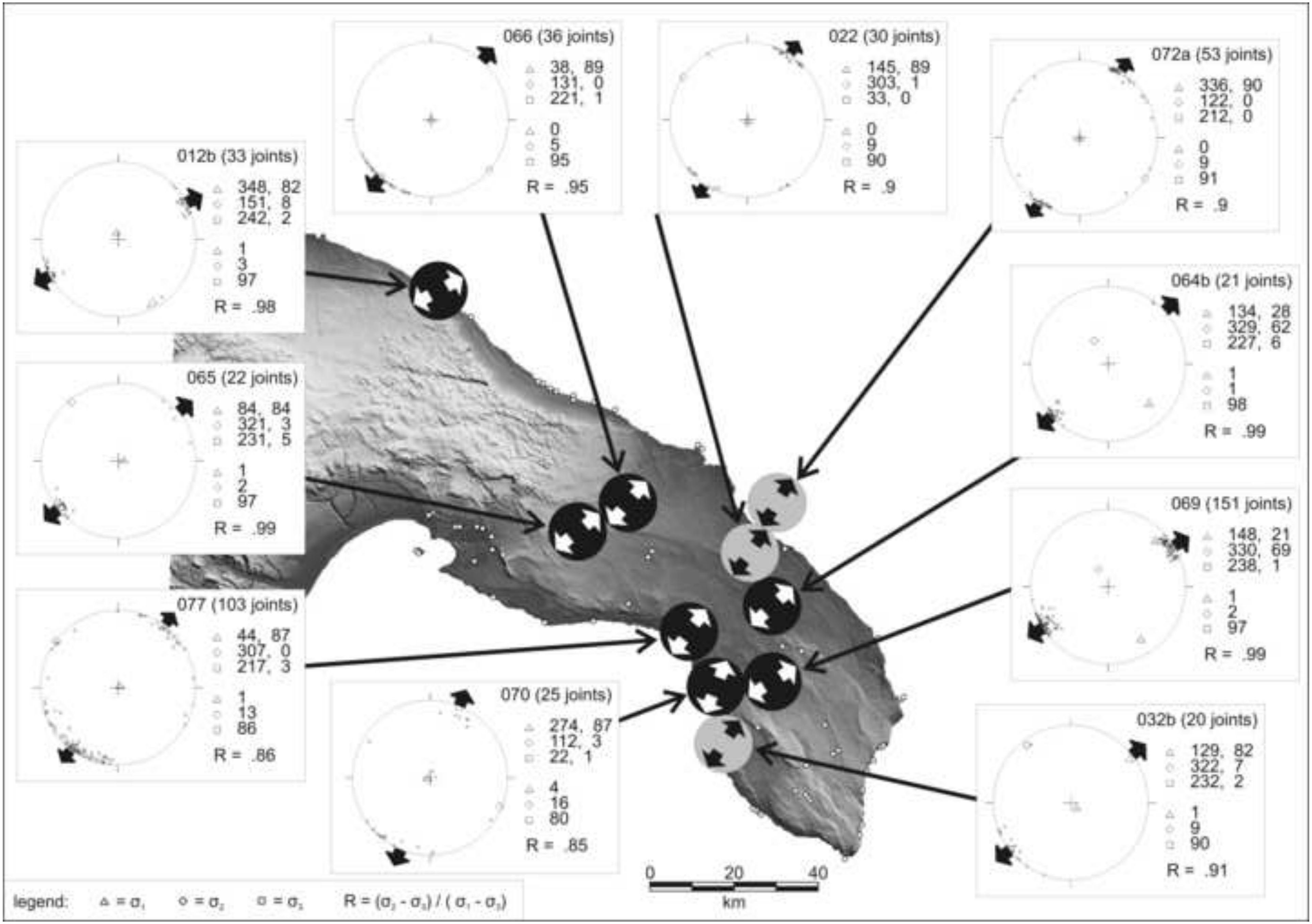

Figure 7c

Click here to download high resolution image

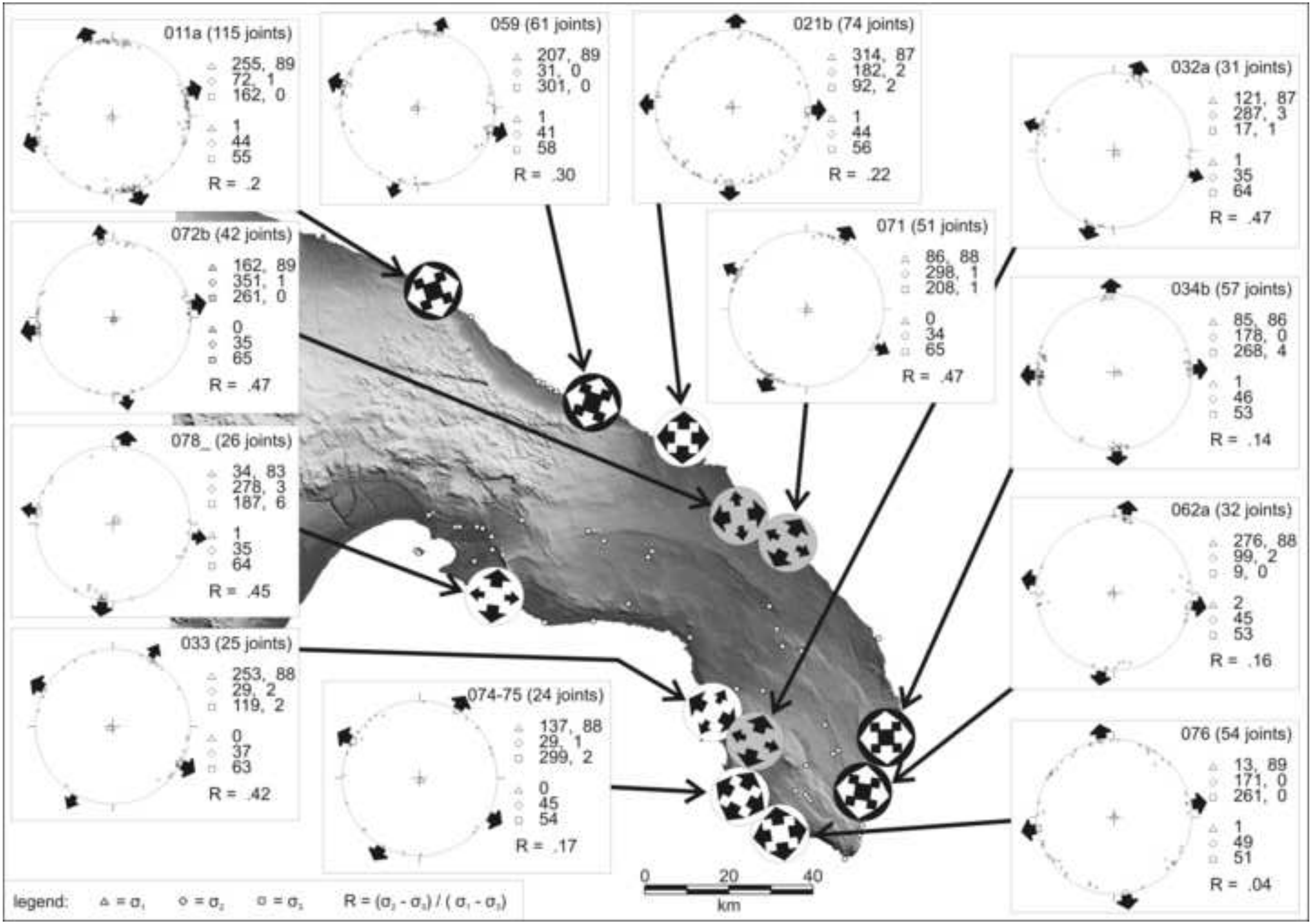

Figure 8
Click here to download high resolution image

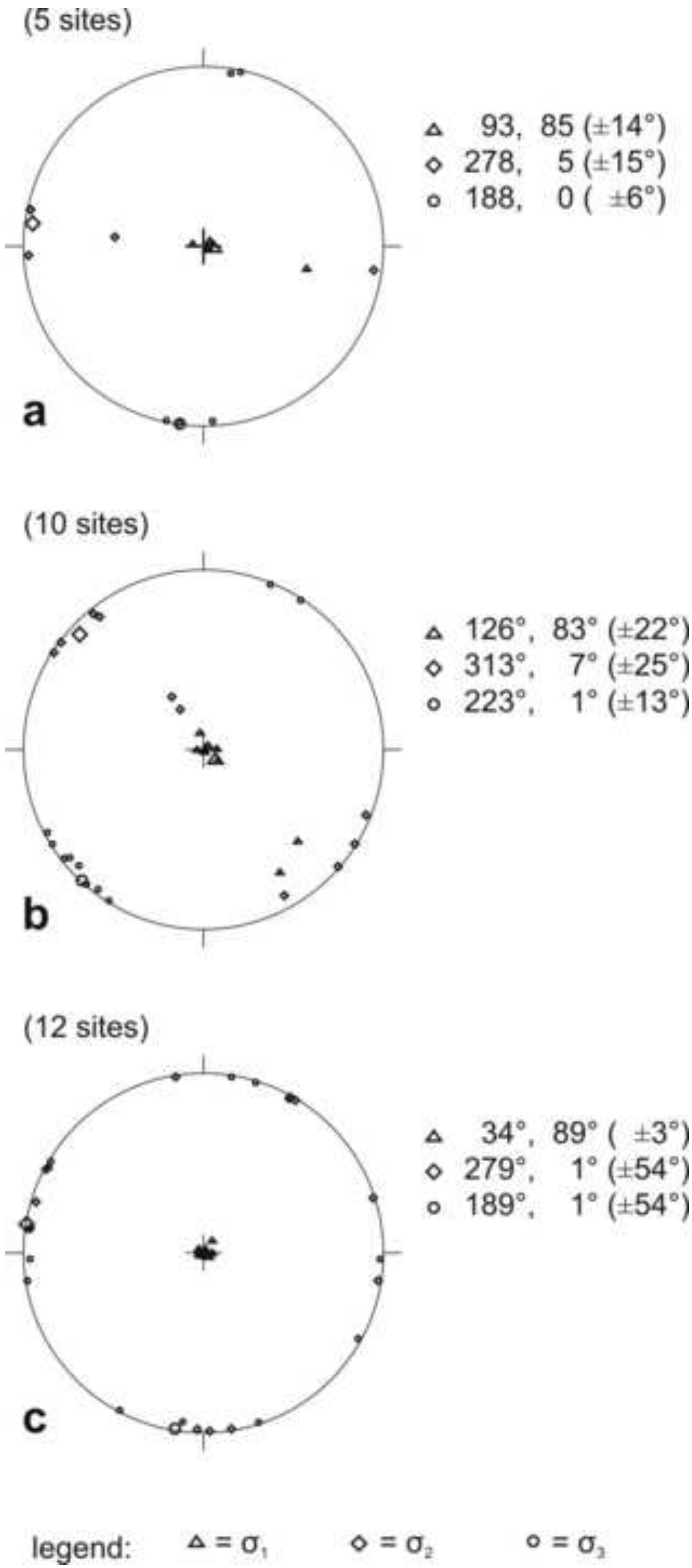

**Figure 9**
**Click here to download high resolution image**